EES Batteries

Accepted Manuscript

This article can be cited before page numbers have been issued, to do this please use: D. Kumar, K. Brijesh, K. Bindu, B. Ramzan, S. Kumar and Z. Khan, *EES Batteries*, 2025, DOI: 10.1039/D5EB00122F.

View Article Online
DOI: 10.1039/D5EB00122F

Broader context

Metal-O_2 batteries are an attractive technology primarily due to their high specific energy. Li-O_2 batteries, for instance, offer the highest theoretical specific energy (~12 kWh/kg), which is comparable to that of gasoline (~13 kWh/kg), making them a promising option for grid and stationary storage applications. However, Li-O_2 batteries suffer from poor efficiency (<60%) and limited rechargeability. In contrast, K-O_2 batteries have demonstrated an energy efficiency of over 90% without the need for an electrocatalyst. This review explores advancements in K-O_2 batteries, covering research on the anode, electrolyte, and electrocatalyst. Additionally, it addresses a key question: "Why does this technology require focused research?"

K-O_2 Batteries: Overcoming Challenges & Unlocking Potential

Divyaratan Kumar,[1,2] Brijesh K,[3] Bindu Kalleshappa,[4] Basharat Ramzan,[5] Surender Kumar,*[5] Ziyauddin Khan,*[1,2]

[1]Laboratory of Organic Electronics, Department of Science and Technology, Linköping University, Norrköping, SE-601 74, Sweden
[2]Wallenberg Wood Science Center, ITN, Linköping University, Norrköping, Sweden
[3]Department of Physics, National Institute of Technology Karnataka, P.O. Srinivasnagar, Surathkal, Mangaluru 575 025, India
[4]Department of Inorganic and Physical Chemistry, Indian Institute of Science, Bangalore – 560012, India
[5]CSIR – Advanced Materials and Processes Research Institute (AMPRI), Bhopal – 462026, India
*Email: surender@ampri.res.in, ziyauddin.khan@liu.se

Abstract:

Batteries have long been a cornerstone of energy storage technologies, offering low-carbon and sustainable solutions across diverse applications from large-scale power grids to electric vehicles and portable electronics. In response to growing global energy demands, research efforts are increasingly directed toward advancing battery chemistries and cell designs to achieve higher performance, efficiency, and scalability. Among emerging systems, potassium–oxygen (K–O_2) batteries have attracted significant attention due to their high theoretical energy density (~935 Wh kg^{-1}) and the earth-abundant nature of potassium. This review presents a comprehensive overview of K–O_2 battery technology, covering fundamental operating principles, key performance limitations, and persistent challenges. Particular focus is given to critical aspects such as electrode architecture, electrolyte stability, and oxygen-related electrochemistry, which collectively govern cell efficiency and durability. In addition, we highlight recent advancements aimed at overcoming these barriers and provide a critical assessment of the current technological readiness of K–O_2 batteries. While the system holds considerable promise, substantial progress is still required to translate laboratory success into practical, real-world applications. Finally, future directions and opportunities for the development and integration of K–O_2 batteries are discussed.

Key words: Metal-O_2, K-O_2, Battery, Efficiency, Energy

View Article Online
DOI: 10.1039/D5EB00122F

1. Introduction

Fossil fuels are an inexpensive and readily available energy source commonly employed to power vehicles. However, uninterrupted consumption of fuels and never-ending energy demand bring us at the verge of consuming all the fossil fuel resources.[1,2] Additionally, there is a climate issue associated with the usage of fossil fuels, which has forced researchers globally to find an environmentally friendly and cost-effective energy source. To combat climate change associated with fossil fuels, electrochemical energy storage devices were regarded as a potential alternative.[3] Two kinds of electrochemical energy storage devices have been known, one is supercapacitors and the other is batteries. Supercapacitors are regarded as power devices, which make the usage of batteries as energy devices advantageous, as they can provide a continuous energy supply on demand.[4] The oil crisis in the 1970s led Prof. Stanley Whittingham, working for Exxon Mobile, to explore the possibility of developing Li-ion battery (LIB) to get rid of fossil fuels.[5] Though the electrochemical properties of lithium were reported in early 1913[6], it took more than 50 years to explore the feasibility of LIB. Further developments made by Prof. John B. Goodenough and Prof. Akira Yoshino led to the successful commercialization of LIB in 1991 by Sony Asahi Kasei teams led by Nishi. Afterwards, the application of LIBs was found in most of the electronic portable devices and household appliances. Despite the emergence of newer battery technologies, LIBs remain dominant in the electronic gadget market due to their high specific energy density of 100-250 Wh kg^{-1}, low density of lithium (0.534 g cm^{-3}), and low standard reduction potential of lithium (-3.04 V vs SHE).[7] Despite its widespread use, the energy density of LIBs remains a limiting factor for their application in electric vehicles (EVs) and hybrid electric vehicles (HEVs), as it typically ranges from 100-250 Wh kg^{-1}, which is considered insufficient.[8] Scientists have turned their attention towards metal-air batteries, including those based on Li, Na, K, Mg, Al, Zn, and Fe due to their impressive specific energy, volumetric energy, and cell voltage, as demonstrated in Figure 1.[9,10,11-13] While researchers have investigated numerous metals from the periodic table for battery applications, alkali metals such as Li, Na, and K offer distinct advantages over other metals in terms of energy density, reaction kinetics, and cost. In this context, metal-oxygen batteries, such as Li-O_2[11], Na-O_2[10], and K-O_2 batteries[14], are grabbing the attention of scientists. The physical properties of the alkali metals (Li, Na and K)[15,16] are listed in Table 1 which compares Li, Na, and K in terms of atomic

number, natural abundance in Earth's crust (ppm), electronic configuration, density, ionic radius, and standard reduction potential.

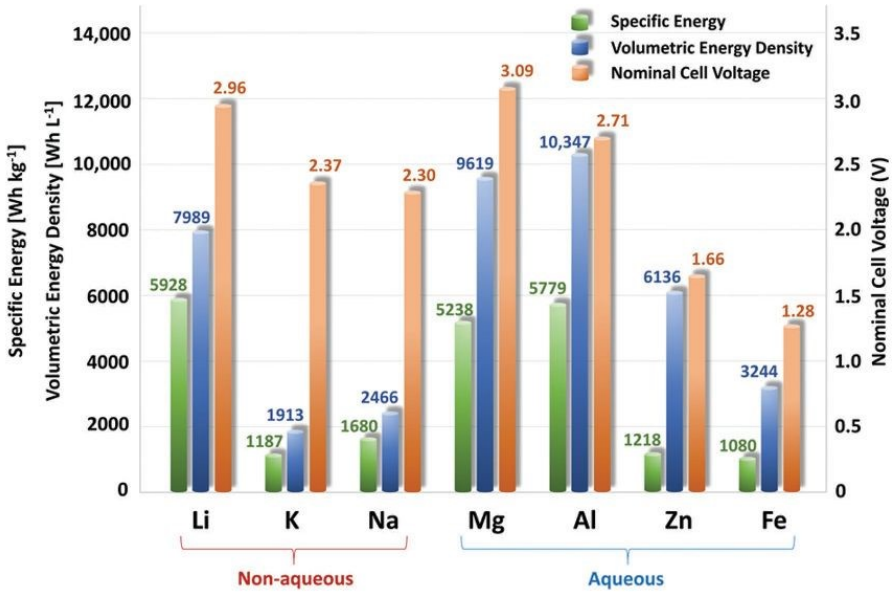

Figure 1: Theoretical energy density, specific energy and cell voltage of the various metal air batteries. Reproduced with permission from [17] Copyright 2016 WILEY-VCH Verlag GmbH & Co. KGaA, Weinheim.

Table 1: Comparison of alkali metals relevant to battery applications.[8, 18]

Alkali metals	Atomic Number	Natural Abundance (ppm)	Electronic shell structure	Density (g cm^{-3}):	Ionic radius (Å)	Reduction Potential (V)
Lithium (Li)	3	18	(2, 1)	0.535	0.76	-3.04
Sodium (Na)	11	22700	(2, 8, 1)	0.968	1.02	-2.71
Potassium (K)	19	21000	(2, 8, 8, 1)	0.858	1.38	-2.93

In particular, Li-O_2 has been sought as a potential candidate for EVs as it provides comparable theoretical specific energy (11680 Wh kg^{-1}) to gasoline.[19] The chemistry of Li-O_2 battery involves the reaction of metallic Li with oxygen, which yields ~2.96 V cell potential and forms lithium peroxide (Li_2O_2) as discharge product via a two-electron process. The main challenges associated with Li-O_2 batteries are the instability of electrolyte, poor specific

View Article Online
DOI: 10.1039/D5EB00122F

capacity, and low round-trip efficiency[20] owing to the sluggish kinetics associated with the Li_2O_2 formation and blockage of oxygen diffusion pathways of air electrode arises from the excessive growth of discharge products (Li_2O_2).[21] It was also found that the cyclic stability of the battery degraded rapidly due to the generation of singlet oxygen ($^1O_2$).[22] Additionally, there are safety and environmental concerns which also limits its large-scale manufacturing.[23] Therefore, searching for a solution beyond Li-based technologies is highly desirable.

Superoxide-based Na-O_2 (1105 Wh kg^{-1} of theoretical specific energy based on NaO_2 discharge product)[24] and K-O_2 (935 Wh kg^{-1} of theoretical specific energy based on KO_2 discharge product)[25] batteries could be a possible alternative to Li-O_2 (3500 Wh/kg of specific energy based on Li_2O_2 discharge product).[26,27] The formation of sodium superoxide (NaO_2) and potassium superoxide (KO_2) involves one electron transfer, which improves the sluggish kinetics associated with oxygen reduction and oxygen evolution reactions, thereby improving the round-trip efficiency and cyclic stability compared to Li-O_2 battery, where the discharge reaction occurred through 2-electron processes.[28] However, the formation of NaO_2 in a non-aqueous media is kinetically preferred but not a thermodynamically stable discharge product. Therefore, NaO_2 further converts into Na_2O_2 (sodium peroxide) either via disproportionation reaction ($2NaO_2 \rightarrow Na_2O_2 + O_2$) or electrochemical reduction reaction ($NaO_2 + Na^+ + e^- \rightarrow Na_2O_2$) leading to low cell reversibility.[29] Moreover, recent studies also showed that the formation of singlet oxygen could be possible reason for the performance degradation of Na-O_2 cells.[30] In contrast to Na-O_2 batteries, KO_2 as discharge product in non-aqueous K-O_2 battery is both thermodynamically stable and kinetically preferred which makes K-O_2 advantages battery system.[25, 31] The fast O_2/KO_2 redox couple guarantee low polarization and also enables the rechargeability of cell well below 3 V vs K/K^+ thus significantly minimizing the formation of singlet oxygen (as the case for both Li-O_2 and Na-O_2 batteries).[14] Moreover, since the rechargeability can be achieved below 3V vs K/K^+ this avoids the participation of parasitic reaction, which typically occurs at higher potentials[28] thereby exhibiting high round-trip efficiency (> 90%). Additionally, K has a higher abundance in earth's crust that can also play a vital role,[32] thereby making K-O_2 batteries a potential alternative to Li-O_2 batteries. The development in this technology is at an early stage and requires more in-depth investigation about electrode/electrolyte interfaces, their effect on reaction kinetics and safety issues. This review emphasises the key aspects of durability and recyclability for battery applications with special reference to challenges involved therein. A detailed discussion about basic cell design, reaction mechanism, novel anode and cathode materials used and their effect on performance

View Article Online
DOI: 10.1039/D5EB00122F

is provided. It concludes with a critical outlook on future research directions and practical advancements in the field of K–O_2 batteries.

2. Cell design and reaction mechanism for metal-air and K-O_2 battery

2.1 Cell reaction of the metal-air battery

Before starting the description, it would be worth to mention that metal-air battery refers air as source of oxygen while metal-O_2 refers pure oxygen as source of oxygen.

The metal-air battery has not been discovered recently; in fact, primary Zn-air battery (typically called Zn-air as it utilises air as a source of oxygen) was first constructed in 1878, which was commercialised in 1932 before the existence of LIBs.[33] In general, metal-O_2 batteries are electrochemical cells which are powered by the oxidation of metal and reduction of oxygen via the oxygen reduction reaction (ORR).[34] In typical design, a metal-O_2 battery consists of a metal electrode as anode, an air cathode commonly known as an electrocatalyst (counter electrode), oxygen/air as cathode and a suitable electrolyte. Alkali metals (Li, Na and K),[35-37] alkaline earth metals (Mg and Ca)[38, 39] and first row transition metals (such as Fe, Zn, etc)[40, 41] can be used as metal anodes for a metal-O_2/air battery. However, electrolyte selection depends on the nature and properties of the metal anode (in Li, Na and K cases, preferably non-aqueous)[40, 41] and cell configuration.[8] The air-breathing cathode should have a porous nature that continuously permits gas flow either from surrounding air or from an oxygen tank. The basic design of any metal-O_2/air battery combines both fuel cell and conventional metal ion batteries. A schematic diagram of metal-O_2/air batteries[42,43] whether non-aqueous or aqueous is shown in Figure 2. During discharge of a metal-O_2/air battery, metal at the negative electrode gets oxidized and generates an electron which moves to the counter electrode (air electrode) where it combines with the oxygen, which gets reduced via ORR. On charge, the metal ion gets deposited on the negative electrode and oxygen evolution takes place at the air electrode. Based on electrolyte, the electrochemical reactions in the cell differ considerably; therefore, discharge products are also different in non-aqueous and aqueous electrolytes. The involved electrochemical reactions on both electrodes can be presented below in aqueous and non-aqueous electrolytes.[43]

In non-aqueous electrolyte

At negative electrode: $M \leftrightarrow M^+ + e^-$ (1)

At air electrode: $xM^+ + O_2 + xe^- \leftrightarrow MxO_2$ (x = 1 or 2) (2)

In aqueous electrolyte

At negative electrode: $M \leftrightarrow M^{n+} + ne^-$ (3)

View Article Online
DOI: 10.1039/D5EB00122F

At air electrode:

$4e^-$ transfer pathway[44]	$O_2 + 4e^- + 2H_2O \leftrightarrow 4OH^-$	(4)
2e- transfer pathway[45, 46]	$O_2 + 2e^- + H_2O \leftrightarrow HO^{2-} + OH^-$	(5)

Metals such as Zn, Fe or Mg can be directly used in aqueous medium, though these metals are thermodynamically unstable and reduce water to produce hydrogen. However, the overpotential for hydrogen reduction can be increased by using various strategies such as using alloyed anode, passivating the surface of metals or modifying the electrolyte, such as water in salt electrolyte[47]. On the contrary, Li, Na and K metals react aggressively with aqueous solution and react violently with water; therefore, they cannot be directly used in aqueous electrolytes. Hence, for the operation of these metals with aqueous electrolytes, the metallic anode is usually protected by an ionic conductive ceramic film known as a solid electrolyte membrane.[48] This solid electrolyte only allows passage of metal ions from aqueous electrolyte to the negative electrode while blocking water.[49] The advantage of aqueous electrolyte is the formation of highly water-soluble discharge products that can avoid the clogging issues (thereby improving the round-trip efficiency and cyclic stability) related to the air electrode in non-aqueous electrolyte. Despite the cell design of these metal-based aqueous batteries being complicated and requiring additional steps, which eventually makes it challenging for large-scale applications.

View Article Online
DOI: 10.1039/D5EB00122F

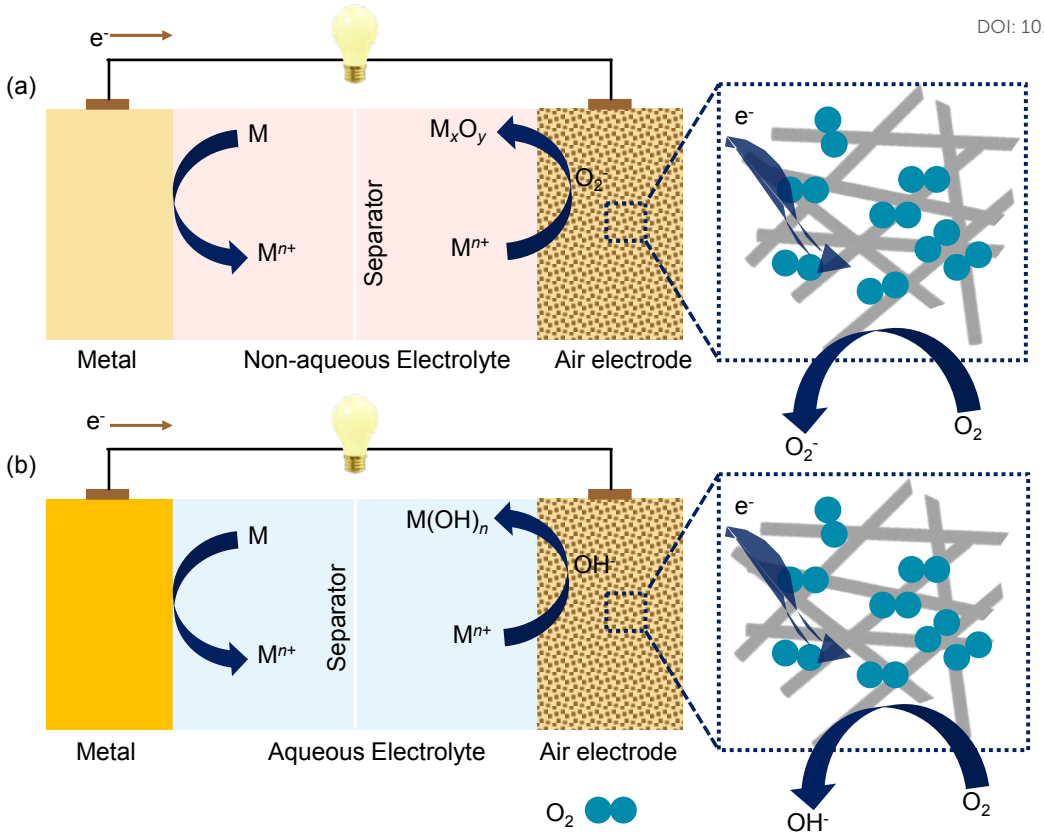

Figure 2: Schematic illustration of (a) metal-O_2 cell in non-aqueous system; and (b) metal-air batteries with aqueous electrolytes.

While it may be easier to fabricate batteries using non-aqueous systems than aqueous ones using alkali metals, their performance is often compromised due to the accumulation of insoluble discharge products that can block the pores of the air electrode. This can lead to poor round-trip efficiency and cyclic stability. In addition, an air electrode requires a membrane which should block moisture and CO_2 from ambient air and only allow passage of O_2. Using this kind of membrane will increase the fabrication cost of the cell, which can pose significant hurdle for practical application. Therefore, it is reasonable to conclude that both types of cells present distinct advantages and limitations, warranting targeted research to overcome their respective challenges.

2.2 Cell components of metal-O_2 batteries

Both metal-oxygen and metal-air batteries typically consist of three main components: an anode, an air cathode, and an electrolyte. The anode is usually made of a metal that can undergo oxidation, such as Li, Na, K or Zn. The air cathode is composed of a porous material that allows

View Article Online
DOI: 10.1039/D5EB00122F

oxygen to enter and participate in electrochemical reactions.[50] Common air cathode materials include carbon,[51, 52] precious metals with carbon,[53, 54] metal oxides,[55, 56] and perovskite-type materials[57]. The cathode of a metal-O_2 battery typically consists of a metallic current collector, a gas diffusion layer, and a coated catalyst. The gas diffusion layer (GDL) serves multiple critical functions: it provides mechanical support for the catalyst layer, enables efficient oxygen transport to the reaction sites, and acts as a barrier to prevent the intrusion of moisture, carbon dioxide, and other contaminants into the battery. A thin, lightweight, porous, and hydrophobic gas diffusion layer effectively bridges the catalyst and oxygen. Additionally, it provides a hydrophobic barrier to prevent electrolyte leakage while maintaining hydrophilic microchannels for enhanced catalytic activity (Figure 2b).[15, 58] A bifunctional catalytic layer is essential at the cathode to improve both the ORR and the oxygen evolution reaction (OER), as oxygen kinetics are inherently slow. Unlike conventional metal-ion batteries, metal-O_2 batteries utilize oxygen directly from the supply.[59] The electrolyte plays a crucial role in ion transport between the anode and cathode. It must be compatible with metal anode and cathode materials while providing sufficient ionic conductivity. Solid-state electrolytes are particularly attractive for metal-O_2 batteries due to their enhanced stability and safety compared to liquid electrolytes.[43]

2.3 Cell design and reaction mechanism of K-O_2 battery

Research on K-metal-based batteries has gained momentum, with early work by Eftekhari et al. in 2004 on K-ion batteries inspiring further exploration of these energy systems.[23] This progress led to the development of the first low-overpotential K-O_2 battery by Ren et al. in 2013, where K^+ ions captured O_2^- to form the thermodynamically stable KO_2 as discharge product.[25] The cell design of K-O_2 battery consists of a K metal anode, a separator with aprotic electrolyte and an air electrode connected with an oxygen reservoir (Figure 3a). Similarly, its cell chemistry involves plating/stripping of K metal on the anode and OER/ORR on the air cathode as presented by equations 6-8.

Anode half-cell reaction: $K \rightarrow K^+ + e^-$ ($E^0 = 2.93$ V) (6)

Cathode half-cell reaction: $K^+ + e^- + O_2 \rightarrow KO_2$ ($E^0 = -0.45$ V) (7)

Overall cell reaction: $K + O_2 \rightarrow KO_2$ ($E^0 = 2.48$ V) (8)

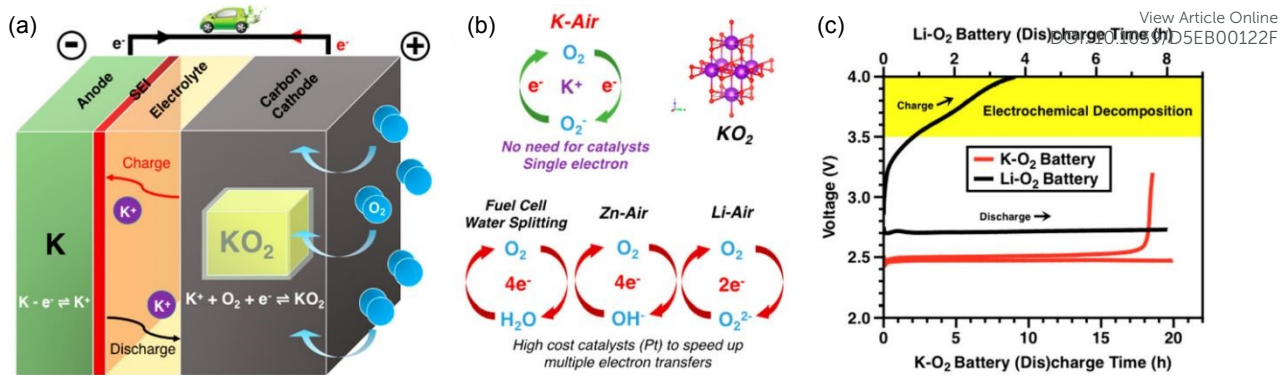

Figure 3: (a) Schematic illustration of K-O_2 battery and discharge process in K-O_2 batteries. (b) Oxygen redox reaction in fuel cell water splitting, Zn-air, Li-air and K-air batteries. (c) comparative charge-discharge profile of Li-O_2 and K-O_2 battery showing the low overpotentials associated with charge-discharge process for K-O_2 battery. Reproduced with permission from [60] Copyright 2018 American Chemical Society.

In Li-O_2 batteries with aprotic electrolyte, reduction of oxygen and reaction of reduced oxygen with Li^+ ions forms LiO_2 a kinetically favoured intermediate that undergoes disproportionation ($2LiO_2 \rightarrow Li_2O_2 + O_2$) or electrochemical reduction ($LiO_2 + Li^+ + e^- \rightarrow Li_2O_2$), to form thermodynamically stable Li_2O_2 which is a two-electron process. Na- and K-metal-based technologies are considered promising alternatives to Li-based systems, owing to their comparable electrochemical properties, greater elemental abundance, and lower material cost. In case of aprotic Na-O_2 batteries, NaO_2 and Na_2O_2 formation have been reported, with Na_2O_2 being thermodynamically favoured, while NaO_2 is the kinetically preferred discharge product.[61] However, no conclusive evidence confirms either as the predominant discharge product.[8] In contrast to both (Li-O_2 and Na-O_2), KO_2 is the sole discharge product in non-aqueous K-O_2 batteries, as it is both thermodynamically stable and kinetically preferred (Table 2 compares different alkali metal and their electrochemical reactions, discharge products, number of electron transferred, cell voltage theoretical specific energy and Gibbs free energy), making K-O_2 batteries an advantageous system (as shown in Figure 3b) as K-O_2 battery operates through one-electron redox process via O_2/O_2^- redox couple. Due to this reason, an effective solution to the persistent kinetic challenges of ORR/OER in oxygen batteries can be achieved without relying on high-performing electrocatalysts.[60] Non-aqueous K-O_2 batteries operate with below 50 mV potential gap at modest current densities lower than aprotic Li-O_2 batteries (Figure 3c), achieving >90% round-trip efficiency due to fast charge transfer kinetics and low overpotential.[25,10] The significantly reduced charging overpotential and high round-trip efficiency are due to the comparable O–O bond lengths in O_2^- (0.128–0.133 nm) and O_2 (0.121

View Article Online
DOI: 10.1039/D5EB00122F

nm), in contrast to O_2^{2-} (~0.149 nm). This suggests a lower reorganization energy and a reduced energy barrier for KO_2 to O_2 conversion, as explained by Marcus Theory.[62]

Table 2: Electrochemical reactions involve in various aprotic alkali metal-O_2 and metal-air batteries

Battery	Overall cell reaction	Discharge product	Number of electrons transferred	Cell voltage (V)	Theoretical specific energy (Wh/kg)	ΔG (kJ/mol)
Li-O_2	$2Li + O_2 \rightarrow Li_2O_2$	Li_2O_2	2	2.96	3458	-570.8
Li-air	$Li + 0.5H_2O + 0.25O_2 \rightarrow LiOH$	LiOH	1	3.45	3860[a] 5796[b]	-332.8
Na-O_2	$2Na + O_2 \rightarrow Na_2O_2$	Na_2O_2	2	2.33	1605	-449.7
	$Na + O_2 \rightarrow NaO_2$	NaO_2	1	2.27	1108	-218.8
Na-air	$Na + 0.5H_2O + 0.25O_2 \rightarrow NaOH$	NaOH	1	3.11	2083[a] 2604[b]	-300.1
K-O_2	$K + O_2 \rightarrow KO_2$	KO_2	1	2.48	935	-239.4

[a]Specific energy was estimated using all reactant Li, Na + $0.5H_2O$ + $0.25O_2$ and one electron
[b]Specific energy was estimated using Li, Na + $0.5H_2O$ reactant and one electron

2.4 Side reactions in K-O_2 batteries and stability of KO_2 discharge product

Though there have been advantages, the side reactions such as corrosion of K metal stimulated by decomposition of electrolyte and oxygen crossover are the primary reasons for the failure of K-O_2 batteries.[63] In K-O_2 batteries, ether-based electrolytes are commonly used, where the oxygen in ether has a chelating ability with metal ions, leading to metal dissolution and consumption. Another issue is the crossover of O_2 from the cathode to the K metal, where it reacts with the K metal, forming KO_2 directly on the anode, thereby leading to the corrosion of the K metal. Ren et al. thoroughly characterised the side reaction on the anode.[63] Then, authors incorporated a polymeric potassium ion-selective membrane (Nafion-K^+) to inhibit the side reactions of K metal using it as a separator. The authors suggested that excellent reversibility can be achieved by using an oxygen–corroded potassium anode. K-O_2 battery using this Nafion-K^+ separator displayed 40 cycles of charge-discharge capability without any increase in charge overpotential (Figure 4a). On contrast, it was observed that the discharge/charge potential gap

View Article Online
DOI: 10.1039/D5EB00122F

increases significantly after the eighth cycle (Figure 4b) in the K-O_2 cell without the K^+ selective separator. With the Nafion-K^+ separator, the cell maintained a relatively stable potential gap (~0.3 V) for over 40 cycles, despite some resistance from the membrane. Additionally, it enhanced coulombic efficiency to over 98% for most cycles.

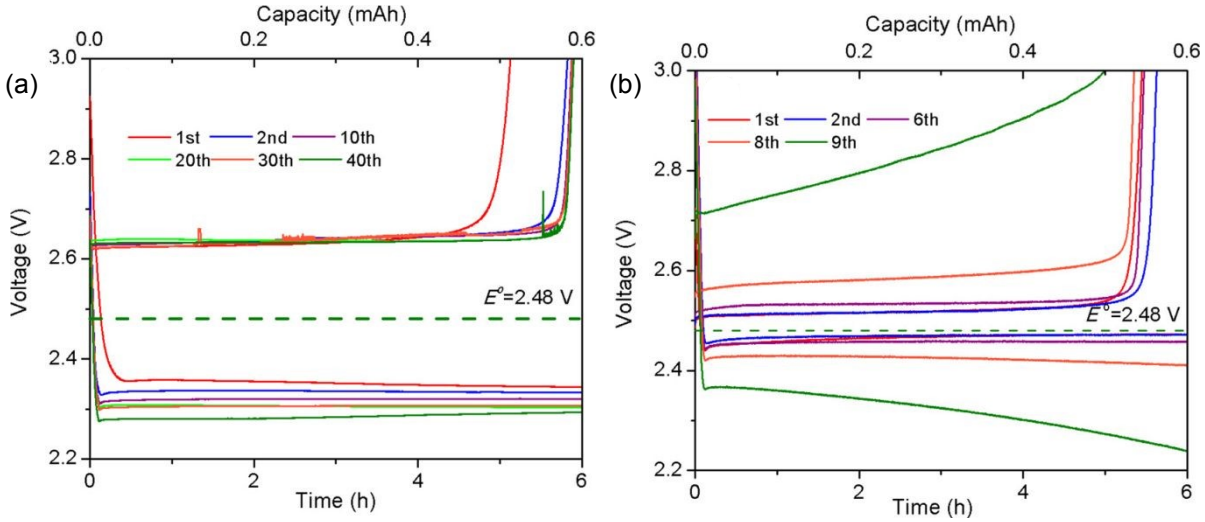

Figure 4: Galvanostatic discharge–charge voltage profiles of K–O_2 batteries (a) with and (b) without a Nafion-K^+ membrane for various cycles. Reproduced with permission from [63] Copyright 2014 American Chemical Society.

Xiao et al. studied the long-term stability of superoxide KO_2 in K-O_2 batteries.[64] Their work explored the KO_2 electrochemistry using various instrumental techniques like chromatography method, SEM and NMR spectroscopy.[63, 64] The reactivity and long-term stability of superoxide in K-O_2 batteries are critical factors. To investigate the long-term stability of KO_2, the authors conducted various experiments to analyse its electrochemistry and the formation of side products resulting from electrolyte decomposition in K-O_2 batteries. Their studies inferred that KF, HCOOK, and a small amount of CH_3COOK and CH_3OCH_2COOK are the major side products of KPF_6 salt and 1,2-dimethoxyethane (DME) solvent. UV/Vis spectroscopy was utilised to study the deleterious effect of parasitic reactions on the coulombic efficiency of K-O_2 batteries. The reversible electrochemical process of KO_2 formation and decomposition at the cathode can prevent excess side reactions in the electrode and electrolyte. However, the growth of KO_2 on the separator after dissolution can lead to a loss of electrons. It has been suggested that the "dead" KO_2 crystals lose their electrical connection with the carbon matrix, similar to the behaviour of Li_2S in Li-S batteries. This loss of connection is believed to contribute to the irreversible portion of K-O_2 batteries. Enhancing the cathode material and its

View Article Online
DOI: 10.1039/D5EB00122F

structure can potentially enhance the KO_2/C contact and reduce the loss of KO_2 in the future. Also, if the resting period of K-O_2 batteries is increased, over-potential increases and voltage fluctuation occur upon charging. This is due to the surface layer growth on the K-anode in the presence of oxygen. On further increasing the resting period, a stable layer of KO_2 is formed on the anode surface, leading to the high coulombic efficiency of the battery.

The investigation conducted by the Yi-Chun Lu group delved into the electrode-electrolyte interface in metal-oxygen batteries,[65] particularly the K-O_2 chemistry, which is crucial in comprehending the reaction mechanism. The study involved the investigation of the reaction mechanism of K-O_2 chemistry at the electrode-electrolyte interface by utilising Ambient Pressure X-ray Photoelectron Spectroscopy (APXPS) to analyse the ORR/OER in ionic liquid-based air batteries (Figure 5a). Besides the commonly accepted one-electron mechanism, the findings showed additional reaction pathways in K-O_2 batteries. The study revealed that the formation and subsequent oxidation of potassium oxide (K_2O) and potassium peroxide (K_2O_2) can trigger irreversible cell reactions, potentially leading to capacity decay in K-O_2 batteries. The research also revealed that impurities such as H_2O and CO_2 in the air can decrease the chemical reversibility of ORR and OER. These findings shed light on the underlying reasons for the irreversible cell chemistry in K-O_2 batteries. Additionally, the study suggests that APXPS analysis of ionic liquid-based air batteries can be a valuable tool to investigate the chemistry of electrode-electrolyte interfaces in metal-air batteries.[65]

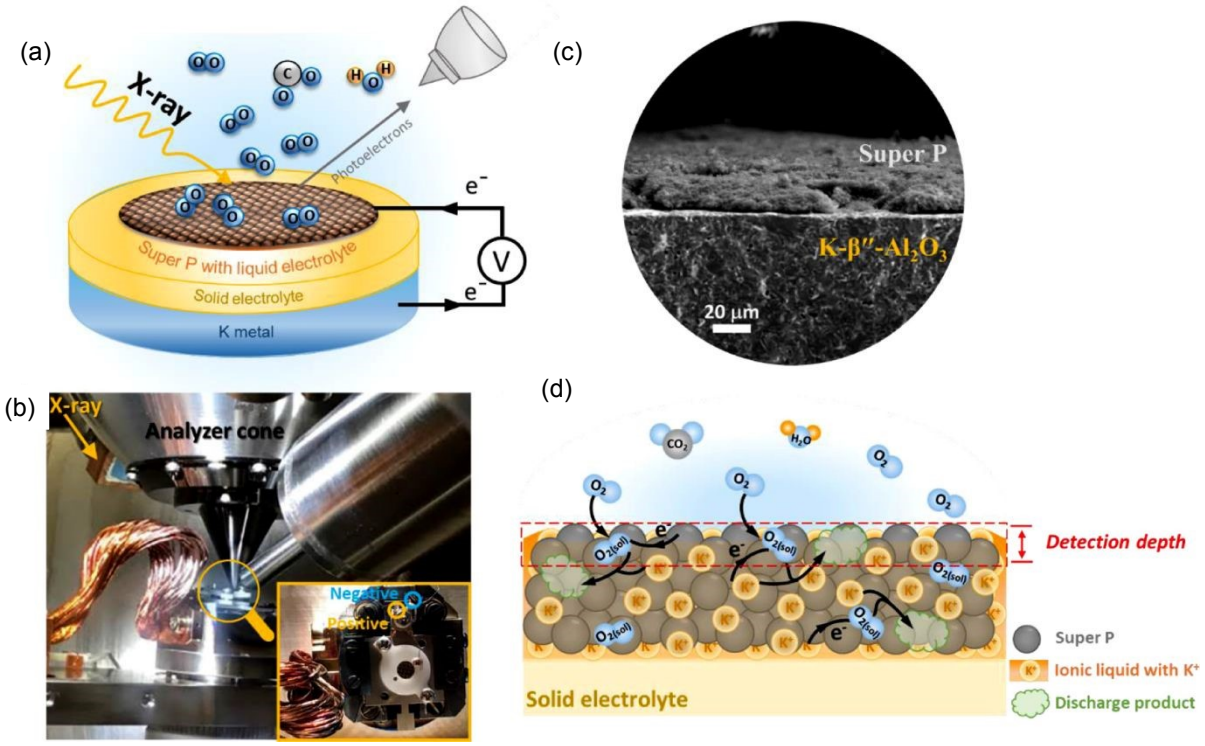

Figure 5: In-situ APXPS measurements conducted on an ionic liquid-based porous K-O_2 battery. (a) the K-O_2 cell, comprising a K metal as anode, K- β'' -Al_2O_3 solid electrolyte, and a Super P carbon as cathode with an ionic liquid electrolyte. (b) Image of the K-O_2 battery during APXPS analysis and (c) SEM cross section of the carbon cathode and solid electrolyte. (d) Schematic of the APXPS sample detection depth, represented by the red dotted area represents. Reproduced with permission from [65] Copyright 2021 Elsevier.

One of the significant findings in this work is the electrochemical reduction of KO_2 to K_2O_2 (Figure 6a and equation 9) when discharging the cell to 1.91 V vs K/K^+. Further lowering the cell discharge potential to 1.12 V vs K/K^+ leads to the formation of K_2O (equation 10). The presence of K_2O_2 significantly reduces the coulombic and charging efficiencies of the K-O_2 battery, affecting its reversibility. Additionally, the formation of K_2O_2 leads to a higher charging overpotential, requiring a higher voltage to charge the battery (Figure 6b). The poor cell performance attributed to K_2O_2 formation may be due to the generation of nucleophilic superoxide anions (O_2^-)[66] or singlet oxygen ($^1O_2$)[67]. The formed O_2^- during the oxidation of K_2O_2 may lead to side reactions, such as attacking cell components or generating reactive singlet oxygen via equation 10.[67] The authors suggested that a higher discharge cutoff voltage (above 2.2 V vs K/K^+) can prevent the formation of K_2O_2 and improve battery reversibility.

$$KO_2 + K^+ + e^- \rightarrow K_2O_2 \qquad (E^0 = 1.91 \text{ vs } K/K^+) \qquad (9)$$

$$K_2O_2 + 2K^+ + 2e^- \rightarrow 2K_2O \qquad (E^0 = 1.12 \text{ vs } K/K^+) \qquad (10)$$

$$2O_2^- + 2H^+ \rightarrow H_2O_2 + {}^1O_2 \qquad (11)$$

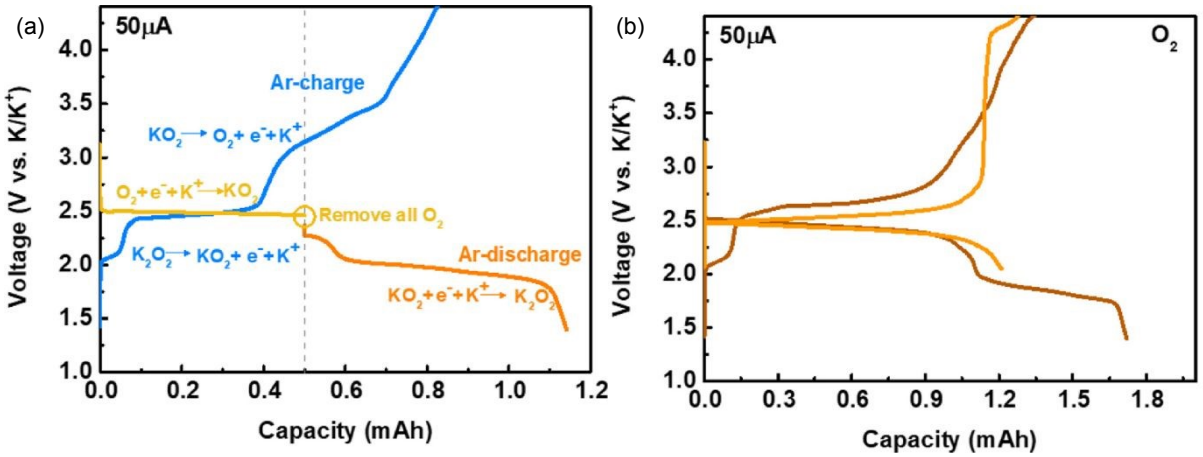

Figure 6: Galvanostatic charge-discharge profile of K-O_2 cell showing conversion of KO_2 to K_2O_2 and its impact on the reversibility of the cell. (a) The cell was discharged up to 0.5 mAh in pure oxygen, and then oxygen was replaced with argon, with continuous discharge followed

View Article Online
DOI: 10.1039/D5EB00122F

by charging the cell under argon gas. (b) Galvanostatic charge-discharge at different cut-off capacities in oxygen atmosphere. Reproduced with permission from [65] Copyright 2021 Elsevier.

In another key study, Küpper et al. investigated the effect of oxygen partial pressure on the discharge behavior and product of K–O_2 batteries by varying the pressure from 0.2 atm to 11 atm.[68] At low pressures (0.2–2 atm), representative of dry ambient conditions, the cells exhibited poor discharge performance and frequent failure due to severe oxygen transport limitations. These limitations led to incomplete cathode utilization, resulting in reduced discharge capacity and rate capability. Furthermore, oxygen depletion triggered parasitic reactions with the DMSO electrolyte, forming byproducts such as K_2SO_4 and K_2CO_3. Discharge profiles under low-to-intermediate pressures showed multistage behavior, indicative of localized oxygen starvation. In contrast, high oxygen pressures (6–11 atm) significantly improved battery performance. A reduction in discharge overpotential by up to 150 mV was observed, along with a 13-fold increase in capacity at a high current density (1.0 mA cm^{-2}) when increasing oxygen partial pressure from 0.2 to 11 atm. Elevated oxygen pressure prevented oxygen depletion, suppressed side reactions, and promoted uniform KO_2 deposition across the cathode. Overall, pressurizing K–O_2 batteries with pure oxygen (≥6 atm) effectively mitigates oxygen transport limitations and electrolyte degradation, thereby enhancing energy efficiency, rate capability, and cycling stability. This strategy offers a promising pathway toward realizing high-capacity, high-rate K–O_2 batteries for practical applications.

View Article Online
DOI: 10.1039/D5EB00122F

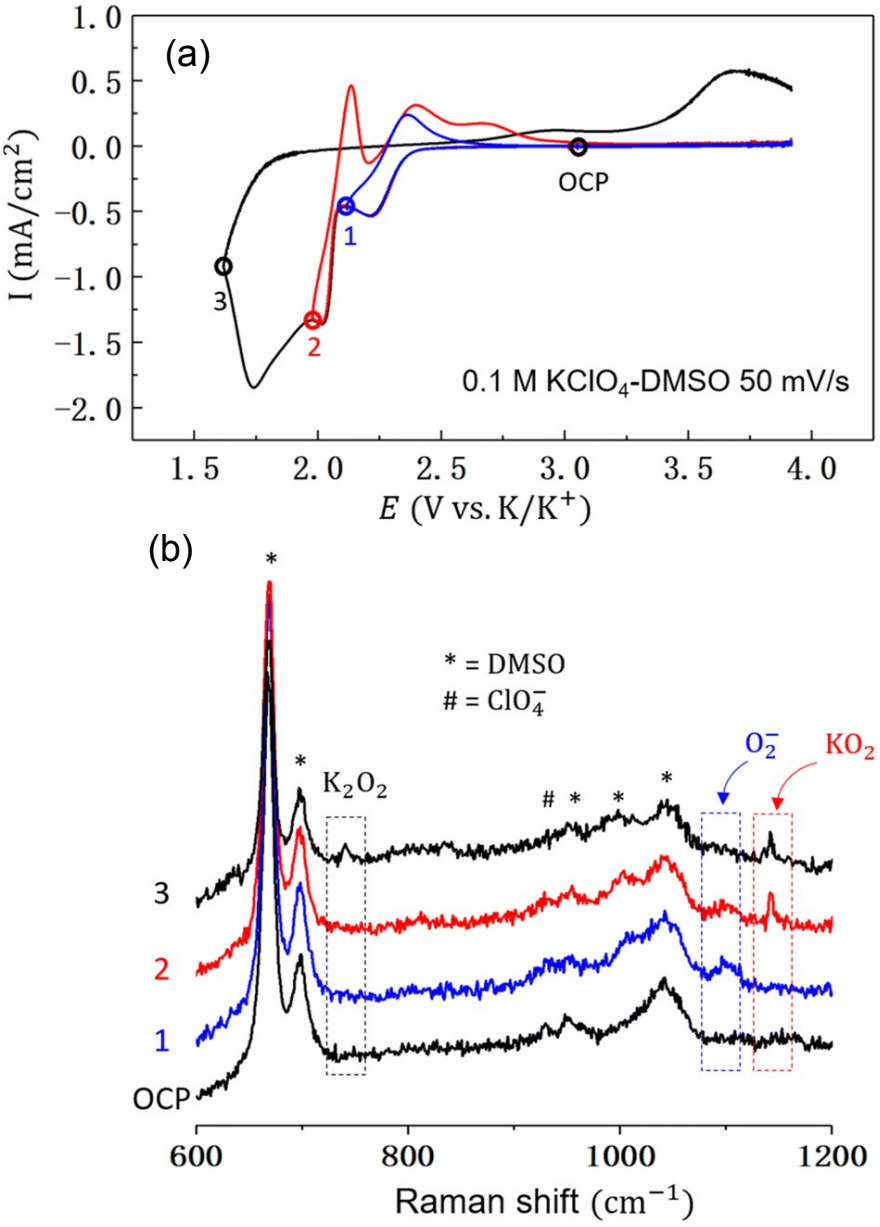

Figure 7: (a) CV recorded in O_2-saturated 0.1 M $KClO_4$ in DMSO electrolyte. (b) Surface-enhanced Raman spectra of the Au electrode at different cut-off potentials and open-circuit potential (OCP). The blue curve corresponds to a cut-off potential of 2.12 V (1), the red to 1.98 V (2), and the black to 1.60 V vs. K/K^+ (3). Reproduced with permission from [69] Copyright 2024 Royal Society of Chemistry.

Liu et al. recently employed in-situ Raman spectroscopy to gain deeper insights into the electrochemistry of K–O_2 batteries, focusing specifically on the oxygen-related redox processes.[69] For this study, the authors used a model system consisting of an Au electrode in a DMSO-based electrolyte. Their findings revealed that the key discharge products are KO_2 and K_2O_2, with superoxide (O_2^-) identified as a critical intermediate whose formation is potential-dependent. At higher discharge potentials (> 1.6 V vs K/K^+), molecular oxygen is first reduced

View Article Online
DOI: 10.1039/D5EB00122F

to an O_2^-* radical anion, which desorbs from the Au electrode surface and enters the solution phase (Figure 7 a & b). There, it reacts with K^+ ions to form KO_2 via a solution-mediated mechanism. In contrast, at lower potentials, oxygen is directly reduced on the Au electrode surface to form an adsorbed KO_2* intermediate, which can be further reduced to K_2O_2* upon deep discharge < 1.6 V vs K/K^+) (Figure 7 a & b). These observations suggest that K_2O_2 is predominantly formed under high discharge overpotentials, and that KO_2 does not undergo a disproportionation reaction during cycling. This study provides important mechanistic insights into the potential-dependent product distribution and electrochemical pathways in K–O_2 batteries.

3. Literature review on K-O_2 batteries

This section provides a concise overview on the development of K-O_2 batteries, including the electrolyte, air cathode, and anode. Each component of cell is crucial in determining life cycle, energy, and efficiency. The electrolyte facilitates ion transport and affects reaction kinetics, making its composition and stability essential for long-term cycling. The air cathode serves as the site for ORR/OER, influencing energy efficiency and discharge capacity. The anode, typically composed of potassium metal or its alternatives, significantly impacts battery lifespan and safety. Understanding the design and optimization of these components is essential for improving K-O_2 battery performance and addressing current challenges.

3.1 Electrolytes for K-O_2 Battery

As is the case with all energy storage devices, the efficient movement of K^+ ions between the electrodes is crucial in K-O_2 batteries, and the choice of electrolyte is crucial as it can significantly affect the stability and performance of the battery, including rate performance, cyclic stability and coulombic efficiency.[70] The ionic transport properties, K^+ ion solvation properties and electrolytes' electrochemical stability greatly affect the batteries' performance. An ideal electrolyte should have high ionic conductivity, low desolvation energy and a large electrochemical stability window. Typically, K^+ ions have weaker interactions (solvation shells) with solvent molecules compared to Li^+ and Na^+ ions due to the larger size, lower charge density and smaller Stokes radii of K^+ ions, thereby enabling rapid ionic transport and higher ionic conductivity.[71] Also, K^+ displayed lower desolvation energy in most of the organic solvents compared to Li^+ and Na^+ ions, which also allows fast migration of K^+ ions (Table 3).[70]

View Article Online
DOI: 10.1039/D5EB00122F

Table 3: Desolvation energy associated with Li^+, Na^+ and K^+ ions in common organic solvents[70, 72]

Solvent	Desolvation energy (kJ/mol)		
	Li	Na	K
Propylene carbonate (PC)	215.8	158.2	119.2
Ethylene carbonate (EC)	208.9	152.8	114.6
Diethyl carbonate (DEC)	205.6	147.9	105.1
Ethyl methyl carbonate (EMC)	199.1	143.1	101.6
Fluoroethylene carbonate (FEC)	188.8	136.2	100.5
Vinylene carbonate (VC)	191.4	138.3	102.2
Butylene carbonate (BC)	219.5	161.4	121.9
Trimethyl phosphate (TMP)	249.1	181.2	135.4
Dimethyl formamide (DMF)	230.1	165.5	122.8
Dimethyl sulfoxide (DMSO)	232.9	167.8	125
N-Methyl-2-pyrrolidone (NMP)	243.6	175.5	131

In metal-O_2 batteries, it has been found that the electrolyte affects the electrochemical performance of the air cathode, especially related to the discharge process. Discharge process can proceed via surface-mediated route or solution-mediated route as shown by equations 12-16.[73-75] These cathode processes involve three phases: solid-liquid-gas, and it is the electrolyte that determines whether the reaction is solution-mediated or surface-mediated.

Surface-mediated route:

$$O_{2(g)} + e^- \rightarrow O_2^-{}_{(surf)} \quad (12)$$

$$O_2^-{}_{(surf)} + K^+ \rightarrow KO_{2(surf)} \quad (13)$$

Solution mediated route:

$$O_2^-{}_{(surf)} \rightarrow O_2^-{}_{(sol)} \quad (14)$$

$$K^+{}_{(sol)} + O_2^-{}_{(sol)} \rightarrow KO_{2(sol)} \quad (15)$$

$$KO_{2(sol)} \rightarrow KO_{2(s)} \quad (16)$$

In general, ester and ether-based electrolytes have been used in potassium batteries.[76] However, it was an ether-based electrolyte which was employed in K-O_2 battery as ether have generally

View Article Online
DOI: 10.1039/D5EB00122F

been considered to be relatively safe with K metal (ethers have less reactive oxygen atoms as they are bonded to two carbon atoms).[77] Moreover, due to the low desolvation process and fast oxygen diffusion kinetics, ether-based electrolytes also provide moderate discharge capacities at moderate current densities.[14, 73] Lastly, ether-based solvent promotes the growth of KO_2 via a solution-mediated route.[78] In the first study on K-O_2 batteries, Ren et al. used 0.5 M KPF_6 dissolved in either DME or a butyl diglyme/diglyme mixture (v/v 2:5) as the electrolyte.[25] This work validated the concept and reversibility of K-O_2 batteries; however, the rechargeability of the cell in this electrolyte was poor, as the cell capacity dropped by nearly half in the second cycle (Figure 8). This degradation was primarily attributed to the diffusion of side products to the metal electrode, forming an insulating layer. Consequently, the charging voltage increased in subsequent cycles compared to the first cycle.

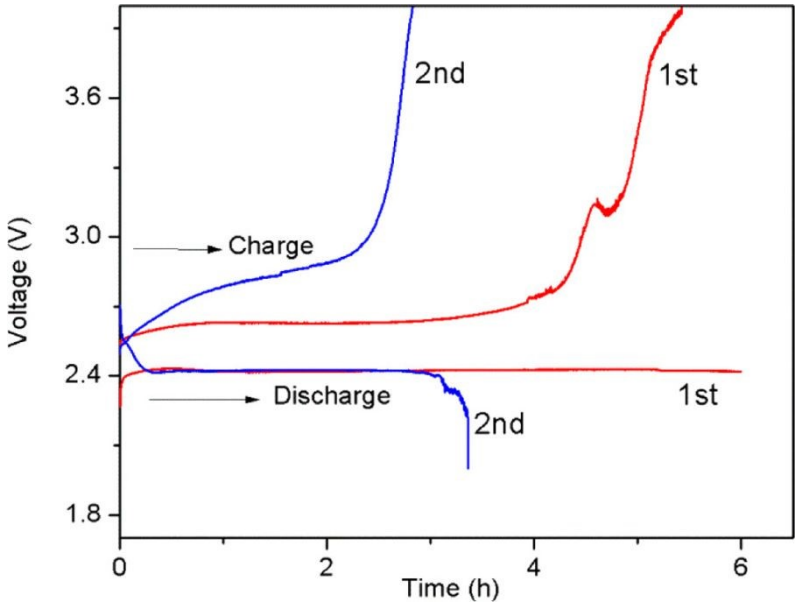

Figure 8: Initial two continuous discharge-charge cycles of the battery at a current density of 0.16 mA/cm^2 in a 0.5 M KPF_6 electrolyte solution composed of butyl diglyme and diglyme (2:5 V/V ratio). Reproduced with permission from [25] Copyright 2013 American Chemical Society.

Wang et al. investigated the reversibility and energy efficiency of K-O_2 batteries in dimethyl sulfoxide (DMSO) and compared it with a diethylene glycol dimethyl ether (diglyme)-based electrolyte (0.5 M KPF_6 in both solvents).[79] They observed that the cell tested in DMSO exhibited higher reversibility and energy efficiency than the one with diglyme. This improvement was attributed to the strong electron-donating ability of DMSO (29.8 kcal/mol donor number)[80] than diglyme (~24 kcal/mol donor number)[81], which stabilizes KO_2, enhancing electrode kinetics and chemical/electrochemical reversibility. The authors emphasized that an

View Article Online
DOI: 10.1039/D5EB00122F

ideal solvent for K-O_2 batteries should strongly stabilize superoxide to ensure fast reaction kinetics and high reversibility. Furthermore, they noted that the lower capacity results from dendritic KO_2 covering the electrode. This issue can be mitigated using a solvent with higher O_2 solubility and lower viscosity, which improves O_2 diffusion, reduces concentration gradients, and promotes cubic KO_2 formation. Sankarasubramanian et al. further proposed DMSO as an effective solvent for the selective production of KO_2, enhancing the rechargeability of K-O_2 batteries.[82] They also observed that the first electron transfer rate constant associated with ORR is four orders of magnitude higher in DMSO compared to ether-based electrolytes, contributing to a significantly improved rate capability. Though DMSO solvent-based electrolytes showed improved reversibility and energy efficiency, surface-confined KO_2 growth and low discharge capacities remain challenges owing to the high desolvation energy barrier of K^+ ions and limited oxygen diffusion. Recent studies highlight the importance of solvent properties and electrolyte structure in improving K-O_2 battery cathode performance.[78] However, an optimized electrolyte design is still needed to enhance capacity and efficiency. The use of a co-solvation strategy that involves DME and DMSO has been demonstrated to decrease the overpotential necessary for cathodic reactions and improve the cathode discharge capacity. The solution-mediated growth of KO_2 and stripping on the cathode surface during cycling were facilitated by the improved solvation structure, which led to a significant improvement in coulombic efficiency for the cathode.[73] A summary of electrolytes utilized in K-O_2 battery has been also provided in Table 4[14] which highlights the current density, capacity, and charge/discharge potential gap across different studies, reflecting variations in electrolyte composition and battery configuration.

Study has also been performed to investigate the kinetics of ORR in KO_2 batteries by using rotating ring-disk electrode (RDE) techniques and differential electrochemical mass spectrometry with DMSO-based electrolytes.[83] DMSO containing K^+ ion, which are credited to the formation of sparingly soluble KO_2 and insoluble K_2O_2 with two reduction processes. The choice of electrode material has been shown to exert a considerable influence on the rate and efficiency of oxygen reduction to superoxide. Specifically, glassy carbon electrodes facilitate this reaction much more readily than gold electrodes, a result that calls into question the conventional assumption of a straightforward outer-sphere mechanism and highlights the importance of electrode surface properties in these processes. The importance of ion pairing between K^+ ions and superoxide, with $KClO_4$ stabilizing superoxide and shifting half-wave potentials to more favorable values compared to electrolytes containing tetrabutylammonium

View Article Online
DOI: 10.1039/D5EB00122F

cation. This has shown to promote significant ion-pairing between superoxide and K^+ ions, resulting in a shift of the half-wave potential toward more positive values. The ion-pairing constant was determined to be $K_{ion} = 7.25 \times 10^2$ mol·L^{-1}. This stabilization effect, quantified by an equilibrium constant for superoxide–K^+ ion pairing, indicates that the influence of potassium cannot be fully explained by conventional Pearson acid-base concepts. Additionally, the presence of water in K-O_2 systems displays a unique effect: isotopic labeling experiments demonstrate that water actually suppresses the formation of K_2O_2, contrary to its role in lithium-based electrolytes. Intriguingly, during oxidation of species deposited on the electrode, an unexpected consumption of oxygen is observed, which has been linked to increased CO_2 evolution, further complicating the picture of how oxygen and potassium ions interact in these advanced battery systems. However, the study suggests that in general K-O_2 battery system is very interesting system as it exhibits well-defined and stable electrochemical behaviour which makes it an attractive candidate for future battery research.

Table 4: List of electrolytes used in K-O_2 battery with capacity and potential gap with cycles

Electrolyte	Current density	Capacity	[b]Potential gap (V)/Cycle	Ref
0.5 M KPF_6 in butyl diglyme/diglyme	0.16 mA/cm^2	0.96 mAh/cm^2	0.25/1; 0.45/2	25
0.5 M KPF_6 in DME	0.065 mA/cm^2	0.39 mAh/cm^2	0.3/1; 0.35/40	63
0.5 M KPF_6 in DME	20 mA/g	0.3 mAh	0.25/1; 0.55/8	84
0.5 M KPF_6 in DME	1 A/g[a] 0.25 mA	1000 mAh/g[a] 0.25 mAh	0.1/1; 0.4/200	75
1 M KTFSI in DME	0.04 mA/cm^2	0.24 mAh/cm^2	0.4/1; 0.4/60	85
0.5 M KPF_6 in diglyme	0.05 mA/cm^2	0.25 mAh/cm^2	0.05/1; 0.4/70	86
0.5 M KPF_6 in DMSO (cathode) 0.5 M KPF_6 in DEGDME (anode)	0.885 mA/cm^2	0.221 mAh/cm^2	0.3/1; 0.55/200	79
0.5 M KPF_6 in DMSO (cathode only)	2 mA/cm^2	0.25 mAh/cm^2	0.53/1; 0.63/2000	87
0.5 M KTFSI in DME/DMSO	0.25 mA/cm^2	4.97 mAh/cm^2	0.04/1; ~0.04/180	73

[a]estimated based on rGO weight. [b]potential gap in first cycle and then gap in the last cycle.

View Article Online
DOI: 10.1039/D5EB00122F

Qin et al. introduced a "solvent-in-anion" strategy to enhance the reversibility of KO_2/K_2O_2 redox reactions in K–O_2 batteries.[88] By incorporating a high-donicity anion additive into a moderately solvating ether-based electrolyte, the authors aimed to modulate electron donicity and stabilize KO_2, thereby enabling catalyst-free, solution-mediated K_2O_2 decomposition. Specifically, the anion additive, (3-methoxypropyl)((trifluoromethyl)sulfonyl)amide ($MPSA^-$), was added to a 0.5 M KPF_6/DME electrolyte, achieving compatibility across the anode–electrolyte–cathode interfaces. This approach established a solution-mediated KO_2/K_2O_2 interconversion pathway with a low overpotential of 216 mV. The K/KO_2 full cell delivered a specific capacity of 292 mAh g^{-1} (based on KO_2 mass), maintained a round-trip efficiency of 84.4%, and operated stably over 120 cycles at 85.4% depth of discharge without an electrocatalyst. Importantly, the cell functioned as a closed, O_2-free system, mitigating gas-related degradation and electrolyte evaporation. Overall, this work demonstrates that high-donicity anions can enable reversible two-electron KO_2/K_2O_2 chemistry without reliance on solid catalysts, offering improved energy efficiency and redox reversibility. However, the study did not investigate the compatibility between high-donicity anions and K metal, which can lead to uncontrolled side reactions at the anode–electrolyte interface and limited full-cell cycle life. Additionally, no strategies were proposed to mitigate K anode corrosion or passivation critical challenges for practical application.[31, 78]

In addition to liquid electrolyte, solid state electrolyte has also been tested for K-O_2 battery to enhance the safety of cell as K metal is highly reactive. To address this, Shao et al. developed a barium-doped K_3SbSe_4 solid-state electrolyte.[89] By substituting Ba^{2+} for K^+, the authors introduced K vacancies, expanded the lattice, and induced a phase transition from trigonal to cubic symmetry. This structural transformation enabled enhanced K^+ ion mobility, resulting in a high ionic conductivity of 0.1 mS cm^{-1} at 40 °C for $K_{2.2}Ba_{0.4}SbSe_4$, over two orders of magnitude higher than the undoped material. The cubic framework facilitated three-dimensional K^+ ion diffusion pathways, significantly reducing interfacial resistance. Using this optimized electrolyte, the authors demonstrated a two-compartment K–O_2 battery separated with solid state electrolyte that operated for 100 cycles without notable degradation, retaining a maximum capacity of ~0.055 mAh with an average coulombic efficiency of 94%. Additionally, the solid-state design effectively prevented oxygen crossover and allowed for the flexible use of different anolytes and catholytes, improving safety and compatibility. Additionally, a water-mediated, super-correlated proton-assisted transport mechanism was

View Article Online
DOI: 10.1039/D5EB00122F

employed to support the feasibility of solid-state K–O_2 batteries, demonstrating stable cycling and enhanced energy efficiency, thereby advancing the development of safer and higher-performing K–O_2 systems.[90] However, the study does not address the long-term chemical and electrochemical stability of water within the solid electrolyte matrix, which remains a critical concern for practical implementation.

The selection of a suitable electrolyte for K–O_2 batteries depends on multiple factors, including electrode materials, targeted performance metrics, and safety and stability requirements. Ongoing research focuses on developing and optimizing electrolyte compositions to enhance the overall performance and reliability of K–O_2 batteries.

3.2. Air cathode for K-O_2 battery

An ideal air electrode in rechargeable metal-O_2 batteries should have a highly porous structure (2–50 nm pore size) to allow efficient oxygen and electrolyte diffusion, as microscopic pores (<2 nm) can block oxygen flow and limit catalytic activity.[21] It must also possess good electrical conductivity to facilitate smooth electron transfer. Additionally, bifunctional catalytic activity is essential, enabling the electrode to efficiently catalyze both charging (OER) and discharging (ORR) reactions. This improves energy efficiency, enhances cycle stability, and reduces energy losses due to high overpotentials. It would be worth saying that most of the research in K-O_2 batteries is focused on the development of electrolytes and understanding the reaction mechanisms of both K metal and air electrodes. Nonetheless, thanks to the electrochemistry of K-O_2 batteries, they do not require high-performance catalysts. This is evident from the fact that most air cathodes tested in K-O_2 batteries are made of carbon-based materials such as Super P carbon black, reduced graphene oxide (rGO), and carbon nanotubes. One such example is the utilization of rGO as a cathode by Xiao et al. to demonstrate high-capacity K-O_2 batteries.[75] A thin, porous rGO cathode has manifold advantages like high specific surface area and pore volume to facilitate oxygen transport and KO_2 deposition. High specific surface area and pore volume of a thin porous rGO cathode facilitate the KO_2 deposition and oxygen transport. Additionally, the high aspect ratio of rGO material provides a large accessible surface area for ORR without any restrictions for pore width. For an rGO-based K−O_2 battery, an overall capacity of more than 8400 mAh g^{-1} is attained at a current density of 1000 mA g^{-1} carbon (Figure 9a). Furthermore, up to 200 cycles with charge and discharge cycles equivalent to more than 400 h were observed as presented in (Figure 9 b & c). By restricting the discharge depth to 1000 mAh g^{-1}, the carbon and rGO electrode battery maintains stable discharge/charge

View Article Online
DOI: 10.1039/D5EB00122F

capacities and coulombic efficiency (~98%) throughout the cycling test. The upsurge of overpotential with the cycle number is mainly due to the oxygen crossover issue in the battery setup. The traversed oxygen is accountable for a thick layer of KO_2 and other by-products on the anode surface. It is fascinating that the rGO-based K−O_2 battery maintains its original high round-trip efficiency. It also shows a considerable enhancement in the cycle number. Besides carbon materials, Zhang et al. recently tested mulberry-like Ag/AgCl@TiO_2/V_2O_{5-x} composite as an air cathode for a long-life K-O_2 battery.[91] The K-O_2 battery exhibited 1392 mAh g^{-1} of discharge capacity with 80 times of long cycle life.

In another strategy, Dou and colleagues introduces an innovative cathode design which is a hierarchical porous carbon nanotube sphere (CNTS) with macropores forming between CNTS and nanopores inside each CNTS for K-O_2 batteries, targeting enhanced cyclic stability, round trip efficiency and rate performance compared to traditional carbon-based cathodes.[92] This architecture enhances cyclic stability, round-trip efficiency, and rate performance compared to traditional carbon-based cathodes. Efficient oxygen diffusion and electrolyte access are promoted throughout the electrode, while the high surface area provides abundant active sites for electrochemical reactions. Comprehensive analyses including coulometry, FTIR, Raman spectroscopy, and XRD reveal a strong correlation between the carbon cathode's structure and the resulting KO_2 morphology, which significantly impacts K–O_2 battery performance. The hierarchical porosity ensures uniform distribution of discharge products and facilitates their decomposition during charging, reducing overpotential and improving energy efficiency. The robust structure accommodates volume changes and resists degradation, resulting in durable long-term operation. Notably, the CNTS cathode showed 2.38 V of average discharge voltage, 95.8% of average coulombic efficiency and stable cycling over 40 cycles with minimal capacity fade. Overall, this study highlights the advantages of tailored porous carbon architectures for advancing K–O_2 battery technology and demonstrates that hierarchical porous carbon nanotube spheres are highly promising for next-generation high-performance energy storage applications.

View Article Online
DOI: 10.1039/D5EB00122F

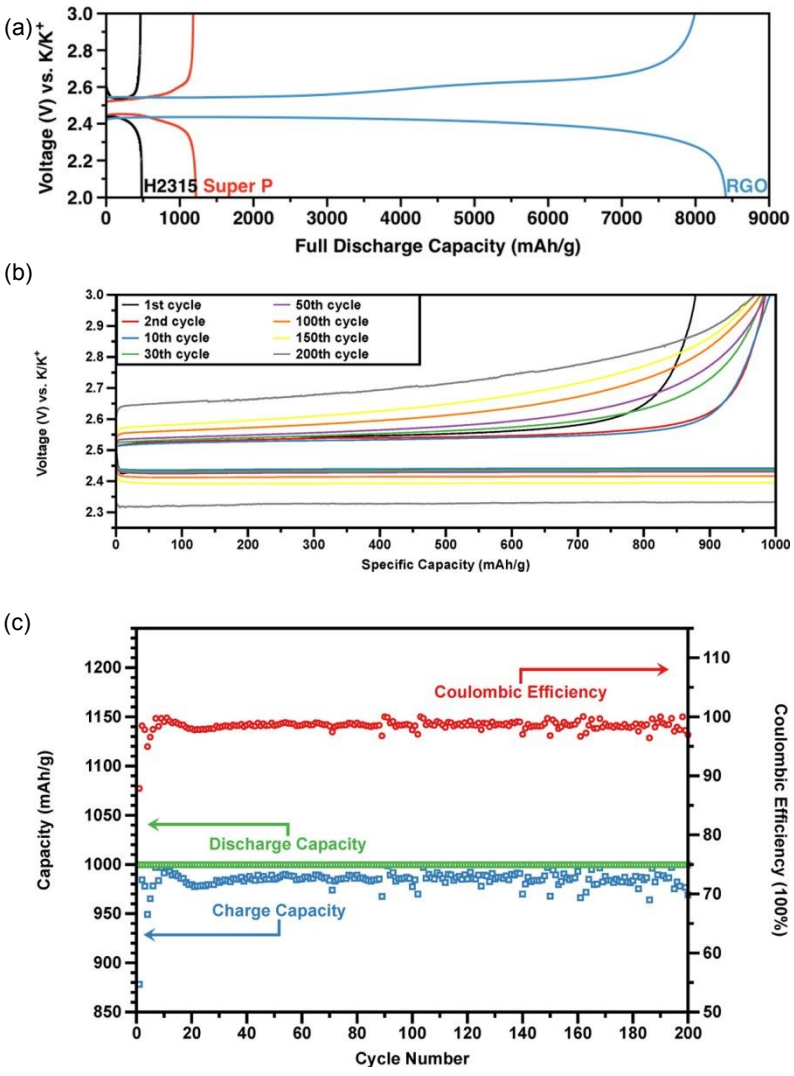

Figure 9: (a) Discharge capacities related with first cycle of carbon fiber electrodes (H2315 Freudenberg FCCT SE & Co. KG), Super P and rGO electrodes; (b) GCD of rGO electrodes upon cycling, (c) Cyclic stability of the rGO electrode at 1000 mA g^{-1} current rate. Reproduced with permission from [75] Copyright 2016 American Chemical Society.

Further, Singh et al. recently proposed a method to enhance cathode performance in K–O_2 batteries through thermal oxidation of carbon paper, commonly used as the air electrode substrate, over varying durations (4 to 24 hours).[93] This treatment yielded a hierarchical porous carbon structure enriched with oxygen-containing surface functional groups. The resulting micro-, meso-, and macro-porosity improved O_2/K^+ transport and increased access to active sites, leading to a significant enhancement in discharge capacity from 3.5 mAh cm^{-2} (untreated) to 5 mAh cm^{-2} (Figure 10a-d). The higher surface area exhibited high charge storage capacity at all current whereas formation of surface O–C=O groups facilitated KO_2 nucleation and improved carbon/electrolyte interfacial stability, thereby reducing the discharge potential by

0.03 V (Figure 10 e-f). This work demonstrates that synergistically engineering cathode porosity and surface chemistry effectively addresses key limitations in oxygen reactivity and ion diffusion, enabling higher capacity and energy-efficient discharge performance. However, the study primarily focuses on discharge behaviour. Critical aspects related to rechargeability such as the evolution of discharge overpotential during cycling, the long-term stability of oxygen-containing groups, and the structural integrity of the porous network under repeated KO_2 formation/decomposition, remain unexplored.

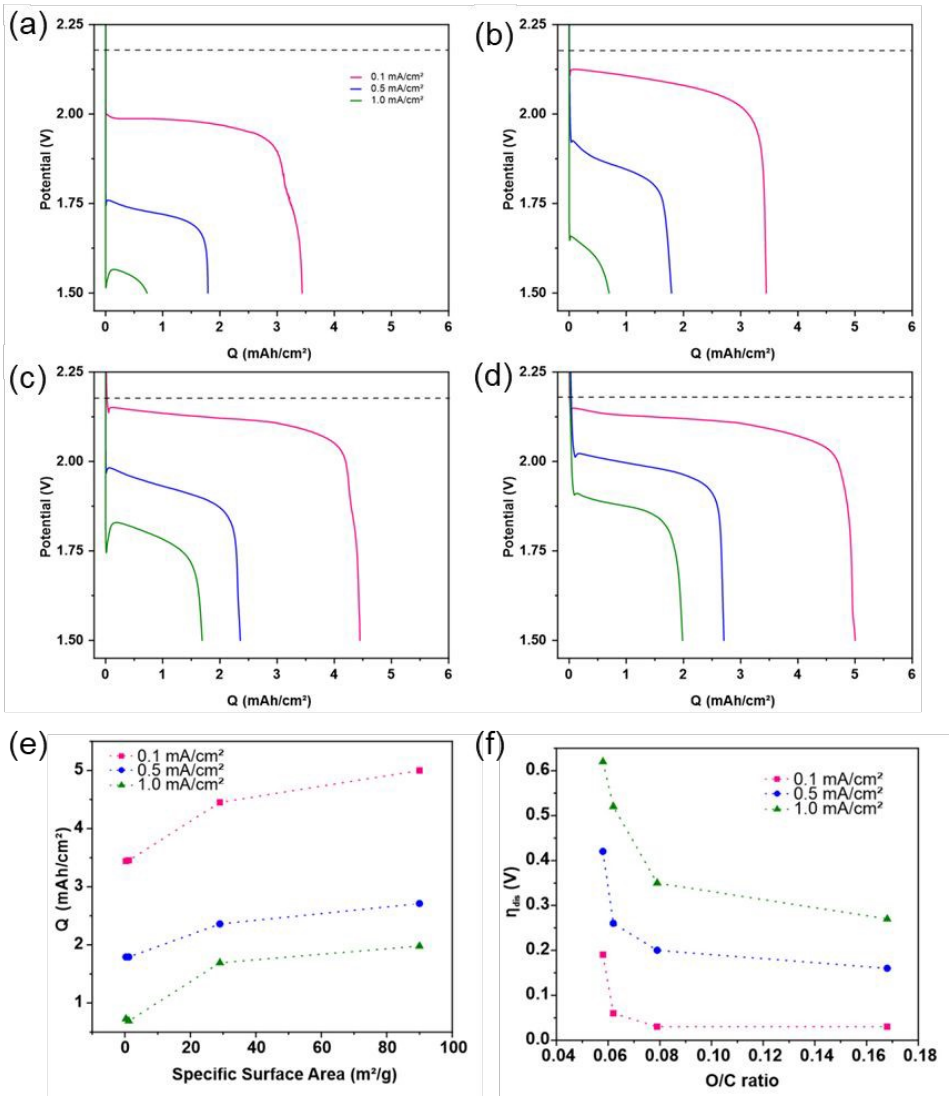

Figure 10: Discharge curve of K-O_2 cell with cathode (a) non-treated, and treated for (b) 4 h, (c) 12 h and (d) 24 h at different current densities (0.1 mA cm^{-2} in pink, 0.5 mA cm^{-2} in blue and 1 mA cm^{-2} in green). The dashed black line in discharge profiles presents open circuit voltage i.e. 2.18 V. Relationship of (e) areal discharge capacity with surface area and (f) discharge overpotential with O/C ratio. The colour coding is same as for discharge profile. Reproduced with permission from [93] Copyright 2024 by the authors. Licensee MDPI, Basel, Switzerland.

View Article Online
DOI: 10.1039/D5EB00122F

Qiao et al. demonstrated that integrating KO_2 into a hybrid catalytic system comprising ruthenium dioxide (RuO_2) nanoparticles anchored on rGO framework enables a non-O_2-evolving, reversible KO_2/K_2O_2 interconversion (Figure 11a).[66] Their investigation identifies O_2^- anion generation as the primary cause of irreversible O_2 release and electrolyte degradation. To address this, they engineered a novel K-deficient $K_{1-x}O_2$–Ru interfacial phase during charging, which effectively suppresses O_2^- anion formation and stabilizes the electrode–electrolyte interface. Transmission electron microscopy (TEM) and XRD analyses confirm the homogeneity of the composite, showing KO_2 nanoparticles (10–15 nm) well-embedded within the RuO_2@rGO matrix (Figure 11b). Electrochemical testing reveals that the RuO_2-free KO_2–rGO cathode (gray curve, Figure 11c) undergoes a sharp potential rise during charging, surpassing the theoretical OER potentials of both K_2O_2 (2.2 V) and KO_2 (2.48 V), indicating irreversible O_2 evolution. In contrast, the KO_2–RuO_2@rGO cathode (blue curve, Figure 11c) exhibits a pronounced and stable discharge plateau at an average voltage of 1.88 V vs. K/K^+, with a minimal overpotential of 0.06 V relative to the theoretical value. This configuration achieves a high specific capacity of 355.6 mAh g^{-1}, corresponding to 94.3% utilization of the theoretical capacity. The optimized half-cell configuration demonstrates exceptional cycling stability, with a minimal average overpotential of 0.2 V and a capacity of 300 mAh g^{-1} (relative to preloaded KO_2 mass) sustained over 900 cycles (Figure 11d). Furthermore, full-cell assemblies incorporating a modified electrolyte and a limited-excess potassium-metal anode achieve outstanding cyclability, rivaling leading potassium-ion battery technologies. This work represents a significant advance in the development of high-capacity, long-life potassium-metal batteries by overcoming the key challenge of irreversible oxygen evolution. However, issues like electrolyte stability towards the reactive O_2^- anion, cost of material and electrocatalyst and K metal issues remains a challenge.

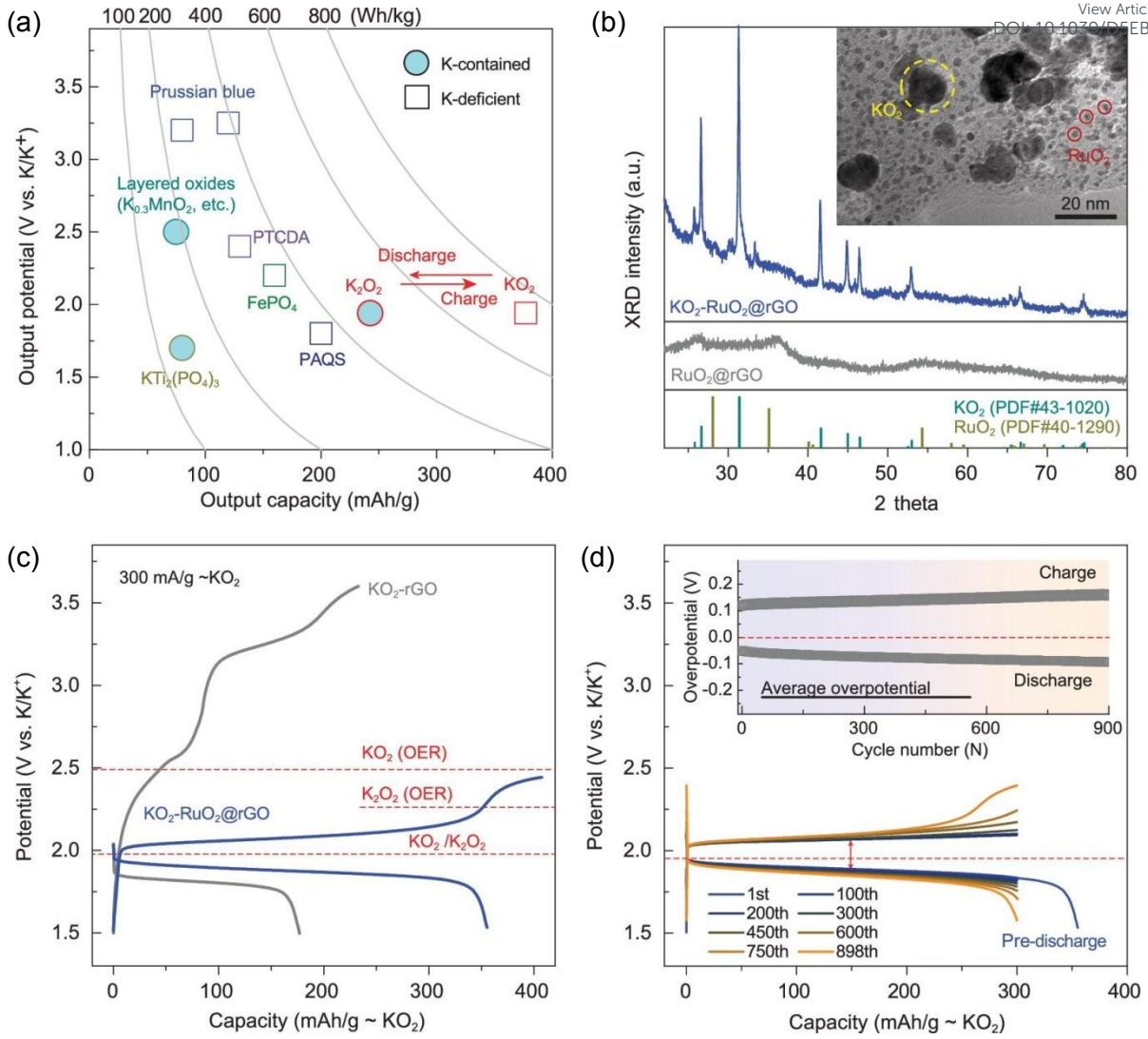

Figure 11: Electrochemical and structural analysis of KO_2-based cathodes in potassium-ion batteries (a) Theoretical comparison of output potential, capacity, and energy density for KO_2 cathodes contrasted with K-ion cathode materials. (b) Material characterization: XRD and TEM of the KO_2-RuO_2@rGO composite, compared with KO_2-rGO. (c) Initial cycle profiles: GCD plot of KO_2-rGO (gray) and KO_2-RuO_2@rGO (blue) cathodes during the first cycle at 300 mA g^{-1}. (d) Half-cell performance: charge-discharge plot of KO_2-RuO_2@rGO with a K metal anode, an average voltage overpotential of 0.2 V (inset) relative to the 1.94 V, current density 300 mA g^{-1}. Reproduced with permission from [66] Copyright 2020, The Author(s) 2020. Published by Oxford University Press on behalf of China Science Publishing & Media Ltd.

3.3. Anode in K-O_2 battery

The role of K metal as an anode significantly affects the performance of K-O_2 batteries, such as energy efficiency and cyclic stability. It has been realised that the reactivity of K metal challenges battery life and safety.[94] Dendritic growth due to repeated cycling, oxygen crossover and electrolyte degradation are the critical issues associated with K metal.[63, 78, 95] These

View Article Online
DOI: 10.1039/D5EB00122F

challenges have led to research on improving and stabilising the anode. To design and develop a high-performance anode, one must comprehend the underlying efficiency parameters, like interfacial chemistry, electrolytic functions, ion diffusion in solid electrodes and correlation between them in K-O_2 batteries.[42] Hence, the main challenges undermining the performance of K-O_2 batteries must be appropriately addressed while designing these batteries. Surface coatings can mitigate any undesirable surface reactions that may persist due to nanostructures with high surface area. McCulloch et al. showed a successful approach to modifying the anode material, resulting in a high-capacity K-O_2 battery.[84] An antimony-based electrode exhibits an average discharge of 1.8 V (Figure 12a) and a reversible storage capacity of 650 mAh/g (98% of the theoretical capacity of 660 mAh/g) corresponding to the formation of a cubic K_3Sb alloy. Antimony has been suggested as a promising anode material for various metal-ion batteries owing to its high theoretical capacity. McCulloch et al. employed a K–Sb alloy anode to demonstrate high-capacity performance in K–O_2 batteries, with reversible cycling capability (Figure 12b). The K_3Sb–O_2 cell exhibited low overpotential and high operating voltage. However, a major limitation arises from the substantial ~407% volume expansion of antimony upon alloying with K, leading to continuous capacity fading. To mitigate this issue, researchers have encapsulated Sb nanoparticles within a carbon matrix to buffer the volume changes. The key advantage of the carbon matrix is its ability to provide an efficient conduction pathway.[34] Hence, the high capacity of Sb/C nanocomposites is attributed to the formation of K_3Sb antimonide. The anodic and cathodic reactions of the K_3Sb-C battery during discharge can be expressed by equations 17 and 18.

At anode

$$K_3Sb \leftrightarrow 3K^+ + 3e^- + Sb \quad (17)$$

At cathode:

$$O_2 + e^- + K^+ \leftrightarrow KO_2 \quad (18)$$

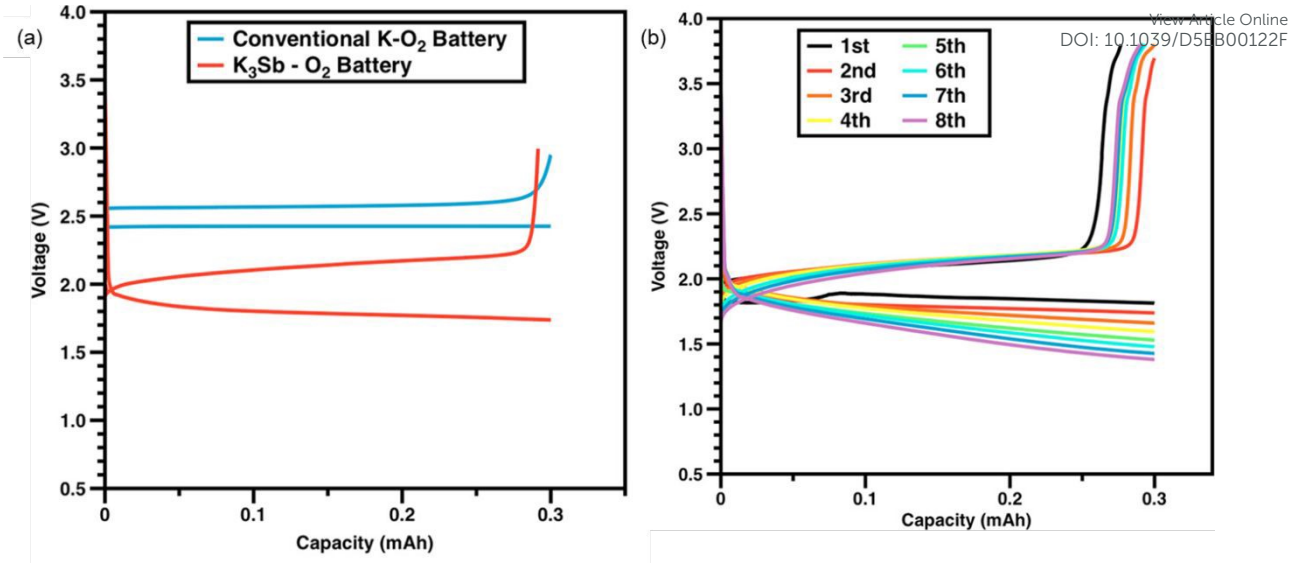

Figure 12: (a) Galvanostatic discharge/charge profiles of a conventional K-O_2 battery and K_3Sb-O_2 battery. (b) Cycling performance of a K_3Sb–O_2 battery. Reproduced with permission from [84] Copyright 2015 American Chemical Society.

The process of charging and discharging results in volume expansion of the electrode, which can cause pulverisation, creating dead areas that are electrically isolated from conductive agents, ultimately leading to capacity fading. To mitigate this issue, a soft and conductive matrix can buffer the volume changes during charging and discharging. In general, to ensure effective interfacial contact, the solvent in the electrolyte of K–O_2 batteries tends to undergo reduction readily on the electrode surface. This possibility might be correlated to the lower redox potential of K^+/K. The lower the initial coulombic efficiency at lower cut-off voltages, the higher the probability of occurrence of side reactions at those voltages. These side reactions are detrimental to battery performance and consume more electrolytes, causing the drying of batteries. Consequently, there is a sharp increase in polarization, thereby degrading the electrode capacity.[96] Dendrite growth is another major problem severely affecting the battery performance as well as their safe usage. Yu et al. suggested a solution by developing a liquid alloy anode for K-O_2 battery.[86] The mechanistic studies for assessing the parameters controlling the capacity and rate performance of metal-O_2 batteries based on superoxide were performed by Xiao *et al.* The possibility of two feasible processes for the growth of KO_2 was proposed. In the first process, K^+ ions from the electrolyte react with reduced oxygen on the cathode surface to form KO_2 crystals. In the second process, electrons transfer through the KO_2 crystal surface and react with oxygen and K^+ ions. The process of formation and distribution of KO_2 is almost like the formation of NaO_2 and Li_2O_2 in Na-O_2 and Li-O_2 batteries respectively, but the

View Article Online
DOI: 10.1039/D5EB00122F

disproportionation step in the Li-O_2 battery is absent for K-O_2 batteries.[97,98] According to the authors, optimizing the cathode materials will be crucial in enhancing the overall capacity and rate capability of K-O_2 batteries. The authors achieved a dendrite-free K-O_2 battery at room temperature using a liquid Na-K alloy, exhibiting a 2.45 V discharge plateau at 0.05 mA/cm^2.[86] A robust and stable liquid-liquid interface was established between the liquid alloy anode and the liquid electrolyte, ensuring high battery performance. The authors also tested this alloy anode in Na-O_2 batteries but found it was only compatible with K-O_2 systems. This was attributed to potassium's stronger reducibility and the formation of the thermodynamically favourable KO_2 over NaO_2 during discharge. The liquid alloy anode enabled a long battery lifespan of up to 620 hours and a low discharge-charge overpotential of 0.05 V. However, challenges such as oxygen crossover and ether-electrolyte instability remain, affecting overall battery performance. Biphenyl-K (BpK) liquid anode was also investigated as an anode in combination with DMSO mediated air cathode.[99] The proposed battery concept showed cyclic stability up to 3000 cycles, with a higher average coulombic efficiency >99.84% at a relatively high current density of 4.0 mA cm^{-2}. This superior performance could be attributed to the suppression in dendritic growth at the anode and minimizing unstable interface and crosstalk between anode, electrolyte and cathode, which includes addressing issues related to oxygen or KO_2 crossover and other chemical reactions between cathode and anode. In addition to these potassiated graphite was also used as anode in K-O_2 battery, which showed reversibility up to 80 cycles with >90% energy efficiencies at a depth of discharge of 25%.[100] In addition to these strategies, potassium graphite intercalation compound was also investigated by Yu Lei and team to address the longstanding challenges associated with metal anodes in K-O_2 batteries, such as severe volume expansion, dendrite growth, and instability due to oxygen crossover.[101] Their strategy was to replace the conventional K metal anode with a graphite intercalation compound (GIC) anode, making both cathode and anode carbon-based materials. Through this novel design, a robust solid electrolyte interphase film was established on the GIC anode, markedly enhancing cycling stability compared to traditional metal K anodes. Notably, the use of a graphite-based anode not only mitigated side reactions triggered by oxygen crossover but also overcame the intrinsic limitations of metal anodes, such as excessive volume change and dendrite formation. This undergoes potassiation/depotassiation at a lower redox potential between 0.8 and 1.0 V (vs. K^+/K), reaching a specific capacity around 110 mAh g^{-1}. The experimental results demonstrated superior electrochemical performance and long-term stability, underscoring the effectiveness of the GIC anode approach.

View Article Online
DOI: 10.1039/D5EB00122F

4. Conclusion and outlook

$K–O_2$ batteries have attracted growing research interest due to the abundance of K metal, improved safety profile compared to $Li–O_2$ systems, and the potential for higher energy efficiency under idealized conditions. While theoretical projections suggest favourable performance, their practical implementation remains constrained by critical challenges such as limited cycle life, parasitic side reactions, and oxygen management. This review highlights recent advances in $K–O_2$ battery development, including progress in electrolytes, air cathodes, anodes, and solid-state electrolytes, with a focus on strategies to mitigate interfacial degradation and enhance long-term stability.

For example, high-donor solvents like DMSO have been shown to enhance O_2/KO_2 redox kinetics and improve cycling stability compared to low-donor solvents like diglyme. While K-O_2 batteries can operate without bifunctional catalysts, rGO cathodes have demonstrated capacities exceeding 8.4 Ah/g with good cycling stability (up to 200 cycles) and high round-trip efficiency. A thin, porous rGO cathode with a high surface area and pore volume facilitates efficient oxygen transport and KO_2 deposition, enabling superior ORR performance. To address safety concerns and prevent dendrite formation, alternative anodes such as K-Sb alloy, Na-K liquid alloy, Bp-based liquid anode and potassium-intercalated graphite have been explored. These materials have shown potential in suppressing dendritic growth, enhancing cycling life, and improving the rate capability of K-O_2 batteries. Though a significant advancement in this area has been made, continued research will be crucial for the practical implementation of K-O_2.

Despite the promising advantages of K-O_2 batteries, several challenges remain, including limited cyclic stability, dendritic growth, lower specific energy and stability issues, which need to be investigated in depth.

i. Finding a suitable electrolyte with enhanced electrochemical stability could help mitigate side product formation and electrolyte consumption. Developing new electrolytes with high donor ability, such as ionic liquids or fluorinated solvents, can improve stability, suppress side reactions, and enhance oxygen solubility for better reaction kinetics. Additionally, highly concentrated electrolyte[102, 103] and localized highly concentrated electrolyte[104] could also be explored for K-O_2 batteries. While high-concentration electrolytes may improve stability, they also bring challenges such as increased viscosity and reduced ionic conductivity. These issues can be partially

View Article Online
DOI: 10.1039/D5EB00122F

addressed using a localized high-concentration electrolyte with a co-solvent strategy. Striking the right balance is crucial for optimising battery performance.

ii. The superoxide-based K-O_2 batteries have demonstrated relatively high energy efficiencies even in the absence of electrocatalysts, highlighting their potential as a next-generation energy storage system. However, significant challenges remain before their practical application can be realized. Nevertheless, the risk to safety and significant side reactions associated with the K metal anode continue to impede its widespread commercialization. Additionally, K metal is prone to dendritic growth, causing short circuits and limiting cycle life. K metal reaction with electrolyte further degrades the solid electrolyte interface, reducing coulombic efficiency and increasing overpotential. Other materials such as potassium-tin alloy, metal sulfides, titanium-based anodes[105] etc. should also be explored.

iii. The air cathode has received relatively less attention and requires further study, as it has been claimed that the cell can be operable without a catalyst. One key issue is the passivation of the cathode surface due to KO_2 formation, which reduces discharge capacity and energy efficiency. Additionally, sluggish OER kinetics can contribute to low round-trip efficiency. Further research is also needed better to understand the kinetics of ORR/OER processes. Exploring high-surface-area carbon materials and metal oxides such as MnO_2,[55] nickel oxides, titanium oxides[106] etc. could help address these challenges. Additional research is also needed better to understand the kinetics of ORR/OER processes.

iv. Oxygen crossover (diffusion of oxygen molecules from the cathode to the anode) and cathode-anode crosstalk (diffusion of reactive species from the cathode to the anode and vice versa), causing corrosion of K metal, are one of the significant challenges in K-O_2 battery. To solve these issues, research should be carried out towards the development of membranes, or solid-state electrolytes, which only allow the transport of K^+ ions and block the other unwanted species. The application of these could improve the safety and cyclic stability of the K-O_2 battery.

v. K metal is highly reactive and has a lower melting point (63.5 °C), which increases the risk of thermal runaway in K metal-based batteries. Therefore, improved cell design and thermal management strategies should be investigated to mitigate the thermal runaway issue and improve the battery lifespan.

vi. Advanced characterization techniques, such as in-situ XRD and XPS, play a crucial role in probing reaction mechanisms and guiding the design of novel materials. The

View Article Online
DOI: 10.1039/D5EB00122F

prediction of electrode material properties can be effectively complemented by computational studies alongside experimental investigations, accelerating technological advancements. To address current challenges in K-O_2 batteries, future research should focus on stabilising discharge products and improving round-trip efficiency to enhance cycling performance. Strategies such as protective coatings or electrolyte additives can help mitigate side reactions, while optimising electrode structures and solvation environments can further enhance efficiency and stability. Ultimately, these advancements could pave the way for the practical adoption of K-O_2 batteries across various applications.

In summary, K-O_2 batteries are a very attractive option for high-energy applications, but they are still far from being a reality. Although some progress has been made, there is significant room for optimization, and much work remains before K-O_2 batteries can become a viable technology.

Acknowledgment:

ZK acknowledges J. Gust. Richert stiftelse for project FunLig BAT (2024-00947) and the Swedish Electricity Storage and Balancing Centre (SESBC) project number MAT2023-21.

References

1. N. Muradov and T. Veziroglu, *International Journal of Hydrogen Energy*, 2008, **33**, 6804-6839.
2. Z. Khan, T. R. Chetia, A. K. Vardhaman, D. Barpuzary, C. V. Sastri and M. Qureshi, *RSC Advances*, 2012, **2**.
3. Z. Khan, D. Kumar and X. Crispin, *Advanced Materials*, 2023, **35**, 2300369.
4. Z. Khan, P. Singh, S. A. Ansari, S. R. Manippady, A. Jaiswal and M. Saxena, *Small*, 2021, **17**, e2006651.
5. K. V. Kravchyk, P. Bhauriyal, L. Piveteau, C. P. Guntlin, B. Pathak and M. V. Kovalenko, *Nat Commun*, 2018, **9**, 4469.
6. G. N. Lewis and F. G. Keyes, *Journal of the American Chemical Society*, 1913, **35**, 340-344.
7. W. Xu, J. Wang, F. Ding, X. Chen, E. Nasybulin, Y. Zhang and J.-G. Zhang, *Energy & Environmental Science*, 2014, **7**, 513-537.

View Article Online
DOI: 10.1039/D5EB00122F

8. Z. Khan, M. Vagin and X. Crispin, *Advanced Science*, 2020, **7**, 1902866.
9. A. V, B. John and M. Td, *ACS Applied Energy Materials*, 2020, **3**, 9478-9492.
10. C. Liu, M. Carboni, W. R. Brant, R. Pan, J. Hedman, J. Zhu, T. Gustafsson and R. Younesi, *ACS Applied Materials & Interfaces*, 2018, **10**, 13534-13541.
11. J. Lu, L. Li, J.-B. Park, Y.-K. Sun, F. Wu and K. Amine, *Chemical Reviews*, 2014, **114**, 5611-5640.
12. D. Kumar, L. R. Franco, N. Abdou, R. Shu, A. Martinelli, C. M. Araujo, J. Gladisch, V. Gueskine, R. Crispin and Z. Khan, *ENERGY & ENVIRONMENTAL MATERIALS*, 2025, **8**, e12752.
13. Z. Khan, D. Kumar, S. Lander, J. Phopase and R. Crispin, *EcoEnergy*, 2024, **2**, 456-465.
14. J. Park, J.-Y. Hwang and W.-J. Kwak, *The Journal of Physical Chemistry Letters*, 2020, **11**, 7849-7856.
15. C. Wang, Y. Yu, J. Niu, Y. Liu, D. Bridges, X. Liu, J. Pooran, Y. Zhang and A. Hu, *Applied Sciences*, 2019, **9**, 2787.
16. L. T. Hieu, S. So, I. T. Kim and J. Hur, *Chemical Engineering Journal*, 2021, **411**.
17. J. Fu, Z. P. Cano, M. G. Park, A. Yu, M. Fowler and Z. Chen, *Advanced Materials*, 2017, **29**, 1604685.
18. J. Zhou and S. Guo, *SmartMat*, 2021, **2**, 176-201.
19. G. Girishkumar, B. McCloskey, A. C. Luntz, S. Swanson and W. Wilcke, *The Journal of Physical Chemistry Letters*, 2010, **1**, 2193-2203.
20. F. Li, T. Zhang and H. Zhou, *Energy & Environmental Science*, 2013, **6**.
21. J. Xiao, D. Mei, X. Li, W. Xu, D. Wang, G. L. Graff, W. D. Bennett, Z. Nie, L. V. Saraf, I. A. Aksay, J. Liu and J.-G. Zhang, *Nano Letters*, 2011, **11**, 5071-5078.
22. G. Houchins, V. Pande and V. Viswanathan, *ACS Energy Letters*, 2020, **5**, 1893-1899.
23. A. Eftekhari, *Journal of Power Sources*, 2004, **126**, 221-228.
24. P. Hartmann, C. L. Bender, M. Vracar, A. K. Durr, A. Garsuch, J. Janek and P. Adelhelm, *Nat Mater*, 2013, **12**, 228-232.
25. X. Ren and Y. Wu, *Journal of the American Chemical Society*, 2013, **135**, 2923-2926.
26. Y.-C. Lu, B. M. Gallant, D. G. Kwabi, J. R. Harding, R. R. Mitchell, M. S. Whittingham and Y. Shao-Horn, *Energy & Environmental Science*, 2013, **6**, 750.
27. W.-J. Kwak, Rosy, D. Sharon, C. Xia, H. Kim, L. R. Johnson, P. G. Bruce, L. F. Nazar, Y.-K. Sun, A. A. Frimer, M. Noked, S. A. Freunberger and D. Aurbach, *Chemical Reviews*, 2020, **120**, 6626-6683.

28. R. Wang, J. Xue, Y. Zhao, R. Zheng and Y. Yang, *Accounts of Materials Research*, 2021, **2**, 447-457.
29. X. Lin, Q. Sun, J. T. Kim, X. Li, J. Zhang and X. Sun, *Nano Energy*, 2023, **112**, 108466.
30. E. Mourad, Y. K. Petit, R. Spezia, A. Samojlov, F. F. Summa, C. Prehal, C. Leypold, N. Mahne, C. Slugovc, O. Fontaine, S. Brutti and S. A. Freunberger, *Energy & Environmental Science*, 2019, **12**, 2559-2568.
31. L. Qin, H. Ao and Y. Wu, *Faraday Discussions*, 2024, **248**, 60-74.
32. J. Sun, Y. Du, Y. Liu, D. Yan, X. Li, D. H. Kim, Z. Lin and X. Zhou, *Chemical Society Reviews*, 2025, **54**, 2543-2594.
33. J.-N. Liu, C.-X. Zhao, J. Wang, D. Ren, B.-Q. Li and Q. Zhang, *Energy & Environmental Science*, 2022, **15**, 4542-4553.
34. A. G. Olabi, E. T. Sayed, T. Wilberforce, A. Jamal, A. H. Alami, K. Elsaid, S. M. A. Rahman, S. K. Shah and M. A. Abdelkareem, *Energies*, 2021, **14**.
35. P. G. Bruce, S. A. Freunberger, L. J. Hardwick and J.-M. Tarascon, *Nature Materials*, 2012, **11**, 19-29.
36. J. M. Munuera, J. I. Paredes, M. Enterría, S. Villar-Rodil, A. G. Kelly, Y. Nalawade, J. N. Coleman, T. Rojo, N. Ortiz-Vitoriano, A. Martínez-Alonso and J. M. D. Tascón, *ACS Applied Materials & Interfaces*, 2020, **12**, 494-506.
37. L. Qin, L. Schkeryantz, J. Zheng, N. Xiao and Y. Wu, *Journal of the American Chemical Society*, 2020, **142**, 11629-11640.
38. G. Vardar, J. G. Smith, T. Thompson, K. Inagaki, J. Naruse, H. Hiramatsu, A. E. S. Sleightholme, J. Sakamoto, D. J. Siegel and C. W. Monroe, *Chemistry of Materials*, 2016, **28**, 7629-7637.
39. P. Reinsberg, C. J. Bondue and H. Baltruschat, *The Journal of Physical Chemistry C*, 2016, **120**, 22179-22185.
40. M. A. Deyab and Q. Mohsen, *Renewable and Sustainable Energy Reviews*, 2021, **139**, 110729.
41. J. Zhang, Q. Zhou, Y. Tang, L. Zhang and Y. Li, *Chemical Science*, 2019, **10**, 8924-8929.
42. W. Zhang, Y. Liu and Z. Guo, *Science Advances*, **5**, eaav7412.
43. Y. Li and J. Lu, *ACS Energy Letters*, 2017, **2**, 1370-1377.
44. H. W. Kim, V. J. Bukas, H. Park, S. Park, K. M. Diederichsen, J. Lim, Y. H. Cho, J. Kim, W. Kim, T. H. Han, J. Voss, A. C. Luntz and B. D. McCloskey, *ACS Catalysis*, 2020, **10**, 852-863.

45. Z. Li, X. Yu, X. Wu, Y. Qiao and S. Ye, *The Journal of Physical Chemistry C*, 2024, **128**, 17878-17885.
46. R. R. Kapaev, N. Leifer, A. R. Kottaichamy, A. Ohayon, L. Wu, M. Shalom and M. Noked, *Angewandte Chemie International Edition*, 2025, **64**, e202418792.
47. Z. Khan, U. Ail, F. Nadia Ajjan, J. Phopase, Z. Ullah Khan, N. Kim, J. Nilsson, O. Inganäs, M. Berggren and X. Crispin, *Advanced Energy and Sustainability Research*, 2022, **3**, 2100165.
48. B. Senthilkumar, Z. Khan, S. Park, I. Seo, H. Ko and Y. Kim, *Journal of Power Sources*, 2016, **311**, 29-34.
49. S. H. Sahgong, S. T. Senthilkumar, K. Kim, S. M. Hwang and Y. Kim, *Electrochemistry Communications*, 2015, **61**, 53-56.
50. F. Cheng and J. Chen, *Chemical Society Reviews*, 2012, **41**, 2172-2192.
51. Y. Wang, R. Yi, W. Fan, G. Li and Q. Yi, *Journal of Power Sources*, 2024, **624**, 235518.
52. Z. Khan, S. O. Park, J. Yang, S. Park, R. Shanker, H.-K. Song, Y. Kim, S. K. Kwak and H. Ko, *Journal of Materials Chemistry A*, 2018, **6**, 24459-24467.
53. S. Zhao, T. Liu, Y. Dai, J. Wang, Y. Wang, Z. Guo, J. Yu, I. T. Bello and M. Ni, *Applied Catalysis B: Environmental*, 2023, **320**, 121992.
54. E. V. Timofeeva, C. U. Segre, G. S. Pour, M. Vazquez and B. L. Patawah, *Current Opinion in Electrochemistry*, 2023, **38**, 101246.
55. Z. Khan, S. Park, S. M. Hwang, J. Yang, Y. Lee, H.-K. Song, Y. Kim and H. Ko, *NPG Asia Materials*, 2016, **8**, e294-e294.
56. Z. Khan, B. Senthilkumar, S. O. Park, S. Park, J. Yang, J. H. Lee, H.-K. Song, Y. Kim, S. K. Kwak and H. Ko, *Journal of Materials Chemistry A*, 2017, **5**, 2037-2044.
57. S. Y. Khan, T. Noor, N. Iqbal and Z. Ali, *Materials Research Bulletin*, 2025, **183**, 113189.
58. J. Qian, Y. Chen, L. Wu, Y. Cao, X. Ai and H. Yang, *Chem Commun (Camb)*, 2012, **48**, 7070-7072.
59. C. Zhou, X. Chen, S. Liu, Y. Han, H. Meng, Q. Jiang, S. Zhao, F. Wei, J. Sun, T. Tan and R. Zhang, *Journal of the American Chemical Society*, 2022, **144**, 2694-2704.
60. N. Xiao, X. Ren, W. D. McCulloch, G. Gourdin and Y. Wu, *Accounts of Chemical Research*, 2018, **51**, 2335-2343.
61. P. Hartmann, C. L. Bender, M. Vračar, A. K. Dürr, A. Garsuch, J. Janek and P. Adelhelm, *Nature Materials*, 2013, **12**, 228-232.

62. Y. K. Petit, E. Mourad, C. Prehal, C. Leypold, A. Windischbacher, D. Mijailovic, C. Slugovc, S. M. Borisov, E. Zojer, S. Brutti, O. Fontaine and S. A. Freunberger, *Nature Chemistry*, 2021, **13**, 465-471.
63. X. Ren, K. C. Lau, M. Yu, X. Bi, E. Kreidler, L. A. Curtiss and Y. Wu, *ACS Applied Materials & Interfaces*, 2014, **6**, 19299-19307.
64. N. Xiao, R. T. Rooney, A. A. Gewirth and Y. Wu, *Angewandte Chemie International Edition*, 2018, **57**, 1227-1231.
65. W. Wang, Y. Wang, C.-H. Wang, Y.-W. Yang and Y.-C. Lu, *Energy Storage Materials*, 2021, **36**, 341-346.
66. Y. Qiao, H. Deng, Z. Chang, X. Cao, H. Yang and H. Zhou, *National Science Review*, 2020, **8**, nwaa287.
67. N. Mahne, B. Schafzahl, C. Leypold, M. Leypold, S. Grumm, A. Leitgeb, Gernot A. Strohmeier, M. Wilkening, O. Fontaine, D. Kramer, C. Slugovc, Sergey M. Borisov and Stefan A. Freunberger, *Nature Energy*, 2017, **2**, 17036.
68. J. Küpper and U. Simon, *Sustainable Energy & Fuels*, 2022, **6**, 1992-2000.
69. J. Liu, L. Guo, Y. Xu, J. Huang and Z. Peng, *Faraday Discussions*, 2024, **248**, 89-101.
70. L. Ni, G. Xu, C. Li and G. Cui, *Exploration*, 2022, **2**, 20210239.
71. S. Dhir, B. Jagger, A. Maguire and M. Pasta, *Nature Communications*, 2023, **14**, 3833.
72. M. Okoshi, Y. Yamada, S. Komaba, A. Yamada and H. Nakai, *Journal of The Electrochemical Society*, 2017, **164**, A54.
73. C. Qiu, J. Jiang, X. Zhao, S. Chen, X. Ren and Y. Wu, *ACS Applied Materials & Interfaces*, 2022, **14**, 55719-55726.
74. C. Xia, R. Black, R. Fernandes, B. Adams and L. F. Nazar, *Nature Chemistry*, 2015, **7**, 496-501.
75. N. Xiao, X. Ren, M. He, W. D. McCulloch and Y. Wu, *ACS Applied Materials & Interfaces*, 2017, **9**, 4301-4308.
76. M. Zhou, P. Bai, X. Ji, J. Yang, C. Wang and Y. Xu, *Advanced Materials*, 2021, **33**, 2003741.
77. H. Wang, J. Dong, Q. Guo, W. Xu, H. Zhang, K. C. Lau, Y. Wei, J. Hu, D. Zhai and F. Kang, *Energy Storage Materials*, 2021, **42**, 526-532.
78. W. Wang and Y.-C. Lu, *Accounts of Materials Research*, 2021, **2**, 515-525.
79. W. Wang, N.-C. Lai, Z. Liang, Y. Wang and Y.-C. Lu, *Angewandte Chemie International Edition*, 2018, **57**, 5042-5046.
80. P. Zhou, Y. Xiang and K. Liu, *Energy & Environmental Science*, 2024, **17**, 8057-8077.

81. N. Ortiz Vitoriano, I. Ruiz de Larramendi, R. L. Sacci, I. Lozano, C. A. Bridges, O. Arcelus, M. Enterría, J. Carrasco, T. Rojo and G. M. Veith, *Energy Storage Materials*, 2020, **29**, 235-245.

82. S. Sankarasubramanian and V. Ramani, *The Journal of Physical Chemistry C*, 2018, **122**, 19319-19327.

83. P. H. Reinsberg, A. Koellisch and H. Baltruschat, *Electrochimica Acta*, 2019, **313**, 223-234.

84. W. D. McCulloch, X. Ren, M. Yu, Z. Huang and Y. Wu, *ACS Applied Materials & Interfaces*, 2015, **7**, 26158-26166.

85. X. Ren, M. He, N. Xiao, W. D. McCulloch and Y. Wu, *Advanced Energy Materials*, 2017, **7**.

86. W. Yu, K. C. Lau, Y. Lei, R. Liu, L. Qin, W. Yang, B. Li, L. A. Curtiss, D. Zhai and F. Kang, *ACS Applied Materials & Interfaces*, 2017, **9**, 31871-31878.

87. G. Gourdin, N. Xiao, W. McCulloch and Y. Wu, *ACS Applied Materials & Interfaces*, 2019, **11**, 2925-2934.

88. L. Qin, L. Schkeryantz and Y. Wu, *Angewandte Chemie International Edition*, 2023, **62**, e202213996.

89. J. Shao, H. Ao, L. Qin, J. Elgin, C. E. Moore, Y. Khalifa, S. Zhang and Y. Wu, *Advanced Materials*, 2023, **35**, 2306809.

90. D.-C. Kong, M. Avdeev, L.-N. Song, L.-J. Zheng, X.-X. Wang and J.-J. Xu, *Energy Storage Materials*, 2024, **72**, 103699.

91. X. Zhang, J. Wang, X. Lang, T. Wang, T. Qu, Q. Lai, L. Li, C. Yao and K. Cai, *Journal of Energy Storage*, 2024, **75**, 109590.

92. Y. Dou, Y. Zhang, F. Guo, Y. Shen, G. Chen, Y. Wei, Z. Xie and Z. Zhou, *Chemical Research in Chinese Universities*, 2021, **37**, 254-258.

93. S. Singh, J. Küpper, A. Abouserie, G. Dalfollo, M. Noyong and U. Simon, *Batteries*, 2024, **10**, 192.

94. P. E. Mason, F. Uhlig, V. Vaněk, T. Buttersack, S. Bauerecker and P. Jungwirth, *Nature Chemistry*, 2015, **7**, 250-254.

95. C. Wei, Y. Tao, H. Fei, Y. An, Y. Tian, J. Feng and Y. Qian, *Energy Storage Materials*, 2020, **30**, 206-227.

96. S. Komaba, T. Hasegawa, M. Dahbi and K. Kubota, *Electrochemistry Communications*, 2015, **60**, 172-175.

97. B. Horstmann, B. Gallant, R. Mitchell, W. G. Bessler, Y. Shao-Horn and M. Z. Bazant, *The Journal of Physical Chemistry Letters*, 2013, **4**, 4217-4222.

98. N. Ortiz-Vitoriano, T. P. Batcho, D. G. Kwabi, B. Han, N. Pour, K. P. C. Yao, C. V. Thompson and Y. Shao-Horn, *The Journal of Physical Chemistry Letters*, 2015, **6**, 2636-2643.

99. G. Cong, W. Wang, N.-C. Lai, Z. Liang and Y.-C. Lu, *Nature Materials*, 2019, **18**, 390-396.

100. L. Qin, S. Zhang, J. Zheng, Y. Lei, D. Zhai and Y. Wu, *Energy & Environmental Science*, 2020, **13**, 3656-3662.

101. Y. Lei, Y. Chen, H. Wang, J. Hu, D. Han, J. Dong, W. Xu, X. Li, Y. Wang, Y. Wu, D. Zhai and F. Kang, *ACS Applied Materials & Interfaces*, 2020, **12**, 37027-37033.

102. T. Hosaka, K. Kubota, H. Kojima and S. Komaba, *Chemical Communications*, 2018, **54**, 8387-8390.

103. N. Ortiz-Vitoriano, I. R. de Larramendi, G. Åvall, R. Cid, M. Enterría, P. Johansson and R. Bouchal, *Energy Storage Materials*, 2024, **70**, 103501.

104. P. Nie, M. Liu, W. Qu, M. Hou, L. Chang, Z. Wu, H. Wang and J. Jiang, *Advanced Functional Materials*, 2023, **33**, 2302235.

105. M. Ma, S. Chong, K. Yao, H. K. Liu, S. X. Dou and W. Huang, *Matter*, 2023, **6**, 3220-3273.

106. S. Karunarathne, C. K. Malaarachchi, A. M. Abdelkader and A. R. Kamali, *Journal of Power Sources*, 2024, **607**, 234553.

View Article Online
DOI: 10.1039/D5EB00122F

Data statement

No new data has been created in this review article.